Frontiers in Bioscience Landmark

Front. Biosci. (Landmark Ed) **2026**; 31(6): 49873
https://doi.org/10.31083/FBL49873

Original Research

Semaglutide Modulates Visceral Adipose Tissue Lipid Metabolism in Type 2 Diabetic Mice: A Lipidomics Study

Xinlei Chen[1], Bingrou Tu[1], Zhaoyuan Li[1], Ping Gao[1], Yi Xu[2,3,*], Yue Yao[1,2,*]

[1]Department of Endocrinology and Metabolism, Second Affiliated Hospital of Harbin Medical University, 150000 Harbin, Heilongjiang, China
[2]Department of Pathology, School of Clinical Medicine, Li Ka Shing Faculty of Medicine, The University of Hong Kong, Hong Kong, China
[3]Department of Hepatopancreatobiliary Surgery, Second Affiliated Hospital of Harbin Medical University, 150000 Harbin, Heilongjiang, China
*Correspondence: xuyihrb@hku.hk (Yi Xu); yaoyue@hrbmu.edu.cn (Yue Yao)

Academic Editor: Paramjit S. Tappia
Submitted: 9 January 2026 Revised: 14 March 2026 Accepted: 10 April 2026 Published: 22 June 2026

Abstract

Background: Type 2 diabetes mellitus (T2DM) is a major public health challenge. This study aimed to explore the molecular mechanisms underlying the effects of semaglutide on lipid metabolism in visceral white adipose tissue in a mouse model of T2DM. **Methods**: Male C57BL/6J mice were given a normal diet, a high-fat diet with streptozotocin, or a high-fat diet with semaglutide. Blood samples, liver tissue, and adipose tissue were collected for analysis. Serum adipokines, inflammatory cytokines, liver function, and lipid profiles were assessed. White adipose tissue and liver sections were processed for hematoxylin and eosin (H&E) staining or immunohistochemistry (IHC) staining for the macrophage marker F4/80. High-throughput targeted lipidomic analysis of epididymal white adipose tissue from these animals was performed using liquid chromatography-tandem mass spectrometry to characterize changes in lipid composition and function. Furthermore, the expression of genes related to adipokines, inflammation, and lipid metabolism in epididymal adipose tissue was determined by reverse transcription-quantitative PCR (RT-qPCR). **Results**: Semaglutide significantly improved systemic metabolism in mice with T2DM, as demonstrated by reductions in body weight, blood glucose, serum lipid levels, and insulin resistance indices homeostasis model assessment of insulin resistance (HOMA-IR) and adipose tissue insulin resistance index (Adipo-IR). Serum Leptin, interleukin-6 (IL-6), and tumor necrosis factor alpha (TNF-α) levels were downregulated, while Adiponectin levels were elevated. Histological analysis revealed that semaglutide effectively reduced adipocyte size, suppressed macrophage infiltration in adipose tissue, and decreased liver lipid accumulation. Targeted lipidomic profiling identified 24 lipid subclasses, of which 50 lipid molecules were significantly changed after semaglutide treatment. Enrichment analysis identified 15 metabolic pathways, with glycerophospholipid metabolism being the most prominently affected. RT-qPCR results confirmed that semaglutide altered the expression of key genes involved in glycerolipid, glycerophospholipid, fatty acid, and cholesterol metabolism. **Conclusions**: These results shed light on the comprehensive remodeling of semaglutide in improving lipid metabolism in epididymal white adipose tissue mice with T2DM.

Keywords: semaglutide; adipose tissue, white; lipid metabolism; diabetes mellitus, type 2

1. Introduction

The global incidence of type 2 diabetes mellitus (T2DM) is rising, affecting over 537 million people worldwide, such that it has become a serious public health challenge [1]. Visceral obesity, the most dangerous type of central obesity, is the main risk factor for obesity and T2DM. A meta-analysis of 216 cohort studies found that every additional 10 cm of waist circumference was associated with a 61% increase in the rate of T2DM incidence, independent of overall obesity [2]. This elevated risk is rooted in the unique pathophysiology of visceral adipose tissue (VAT). VAT exhibits heightened lipolytic activity, releasing excessive free fatty acids (FFAs) that drive systemic lipotoxicity [3]. Lyu et al. [4] demonstrated that VAT develops intrinsic insulin resistance through lipid-induced signaling defects, specifically involving plasma membrane sn-1,2-diacylglycerol accumulation that activates protein kinase C (PKC)ε, leading to impaired insulin receptor phosphorylation. Metabolic disorders induced by VAT are also compounded by chronic inflammation, characterized by the recruitment of pro-inflammatory M1 macrophages that form crown-like structures and secrete cytokines such as tumor necrosis factor alpha (TNF-α), further inhibiting insulin signaling via JNK activation [5]. Collectively, these results indicate the central role of VAT in the lipid metabolism disorders of T2DM, suggesting that specifically targeting VAT could offer significant therapeutic potential.

Glucagon-like peptide-1 (GLP-1) is an endogenous incretin that is involved in glucose and lipid homeostasis through receptor-mediated signaling. Glucagon-like peptide-1 receptor agonists (GLP-1RAs) are widely used as clinically effective first-line therapy for glycemic control and body weight management [6]. In addition to the classic glucoregulatory and weight-loss effects, GLP-1RAs have been shown to improve lipid profiles, decrease liver enzyme levels, reverse metabolic liver disease, improve outcomes in patients with complex metabolic disorders, and reduce long-term diabetic complications in clinical studies [7,8].

Semaglutide is a long-acting GLP-1RA that has received high levels of clinical and research interest owing to its potent effects on obesity, T2DM, and metabolic dysfunction-associated fatty liver disease. Relative to other GLP-1RAs, semaglutide exhibits a pronounced ability to significantly reduce the levels of VAT, which is crucial given that this remains the main risk factor associated with T2DM and obesity. However, the molecular mechanisms underlying the ability of semaglutide to regulate visceral adipose tissue lipid composition and remodeling in T2DM remain poorly understood.

In this study, we investigated the effects of semaglutide on lipid composition and metabolism in visceral white adipose tissue by integrating targeted lipidomics analyses together with the evaluation of lipid metabolism-related gene expression, relevant metabolic indicators, and histopathological indicators. A T2DM mouse model was induced by administering a high-fat diet (HFD) supplemented with streptozotocin (STZ), after which systemic metabolic parameters and histopathological changes were conducted in these animals, followed by targeted lipidomic analysis to characterize changes in lipid composition. Finally, correlations between differentially abundant lipid molecules, metabolic indicators, and gene expression profiles were examined.

2. Materials and Methods

2.1 Animal Models

C57BL/6J mice (male, 6–8 weeks old) were purchased from Beijing Vital River Laboratory Animal Technology Co., Ltd. (C57BL/6J, Beijing, China) and were maintained at the Center for Animal Experimentation of the Second Affiliated Hospital of Harbin Medical University under controlled conditions (25 °C, 12:12-hour light-dark cycle) with free access to food and water. After one week of acclimatization, mice were randomly divided into two groups: a normal diet group (CON, n = 7) and a high-fat diet group (HFD, fed a diet containing 60% fat, D12492, Xiaoshu Youtai Company, Beijing, China). After 4 weeks of HFD feeding, mice in the HFD group underwent a 12-hour fast (with access to water), and a one-time intraperitoneal injection of streptozotocin (STZ, 100 mg/kg, S6050F, Biotopped Technology Co., Ltd. Beijing, China prepared in sodium citrate buffer, C1013, Solarbio Science & Technology Co., Ltd., Beijing, China) was administered [9]. Three days after the injection, blood glucose was measured. The criteria for successfully establishing a T2DM model were: random blood glucose levels greater than 16.7 mmol/L or fasting blood glucose levels greater than 11.1 mmol/L. After blood glucose levels stabilized, the diabetic model mice were randomly assigned to two groups: one group of mice received subcutaneous injections of semaglutide (SJ20210014, Novo Nordisk, Copenhagen, Denmark) at a 60 μg/kg/d dose (HFS group, n = 7), while the other (HFD group, n = 7) received subcutaneous injections of an equal volume of PBS (SC106, Saiwen Innovation Biotechnology Co., Ltd., Beijing, China). Weekly measurements of weight and blood glucose during the 8-week treatment period. This research has been reviewed and approved by the Medical Ethics Committee of the Second Affiliated Hospital of Harbin Medical University, Heilongjiang Province. Animal experimentation procedures strictly adhere to approved experimental protocols and ethical guidelines.

2.2 Tissue Harvesting

Mice were given 1% sodium pentobarbital (60 mg/kg, P3761, Sigma-Aldrich, Merck KGaA, Darmstadt, Germany) for anesthesia after being fasted for 12 hours (with access to water). Blood samples were collected and allowed to clot for 2 hours at room temperature. Then, the samples were centrifuged at 3000 g for 15 minutes at 4 °C. The serum was subsequently stored at –80 °C for further use. After blood collection, the mice were euthanized via decapitation. Before excising the liver, residual blood was flushed by perfusing with PBS injected via the portal vein, after which the liver was removed and immersed in 4% paraformaldehyde (SI101-01, Saiwen Innovation Biotechnology Co., Ltd., Beijing, China) for fixation prior to hematoxylin-eosin (H&E) staining. Visceral adipose tissue (epididymal, perirenal, and mesenteric fat) and subscapular brown adipose tissue were weighed and collected for further analysis. Epididymal adipose tissue was subjected to H&E staining and immunohistochemistry for F4/80 (28463-1-AP, Proteintech Group, Inc., Wuhan, China). The entire euthanasia process was performed in strict adherence with the operating procedures approved by the Medical Ethics Committee of the Second Affiliated Hospital of Harbin Medical University, Heilongjiang Province, ensuring animal welfare.

2.3 Intraperitoneal Glucose Tolerance Test (IPGTT)

All mice were weighed after 12 hours of fasting and administered a 50% glucose injection (2 g/kg) via intraperitoneal injection. Blood glucose levels were measured at 0 min (pre-injection), 30, 60, 90, and 120 minutes post-injection, after which blood glucose response curves were constructed, and the area under the curve (AUC) was measured.

2.4 Serum Analysis

The collected serum samples were used to measure liver function indicators in these experimental mice, including levels of alanine aminotransferase (ALT), aspartate aminotransferase (AST), and lipid-related indicators, high-density lipoprotein cholesterol (HDL-C), low-density lipoprotein cholesterol (LDL-C), total cholesterol (TC), and triglycerides (TG). All these parameters were analyzed by testing performed in the Clinical Laboratory Department of the Second Affiliated Hospital of Harbin Medical University for testing.

2.5 Enzyme-Linked Immunosorbent Assay (ELISA)

Serum levels of interleukin-6 (IL-6), tumor necrosis factor alpha (TNF-α), Leptin, Adiponectin, and insulin in mice were measured using commercial ELISA kits (Shanghai Jonlnbio Industrial Co., Ltd.). Based on the provided kit instructions, 100 µL of diluted sample was added to precoated microtiter plates, adding an equal volume of universal diluent to blank wells, followed by incubation at 37 °C for 1 hour. After washing, 100 µL of the biotin-labeled antibody working solution was added per well, followed by a further incubation at 37 °C for 1 hour. The wells were then washed again, followed by the addition of 100 µL of enzyme-labeled working solution, and incubation at 37 °C for 30 minutes. After 5 washes, TMB substrate (90 µL) was added to each well, and plates were incubated at 37 °C in the dark for 15 minutes. Then, stop solution (50 µL) was added to terminate the reaction, and absorbance at 450 nm was measured using a microplate reader. The utilized ELISA kits were as follows: Leptin (JL11317-96T, Jonlnbio Industrial Co., Ltd., Shanghai, China), Adiponectin (JL20696-96T, Jonlnbio Industrial Co., Ltd., Shanghai, China), IL-6 (JL20268-96T, Jonlnbio Industrial Co., Ltd., Shanghai, China), TNF-α (JL10484-96T, Jonlnbio Industrial Co., Ltd., Shanghai, China), and Insulin (JL11459-96T, Jonlnbio Industrial Co., Ltd., Shanghai, China).

2.6 Serum Free Fatty Acid (FFA) Assay

An FFA content assay kit (AKFA008M, Beijing Boxbio Science & Technology Co., Ltd., Beijing, China) was used as directed. Serum samples were extracted with the provided extraction reagent, and the provided solution was used for measurement. Briefly, 200 µL aliquots of the extracted reaction solution were dispensed into a 96-well plate, establishing appropriate test, control, standard, and blank wells. Absorbance was then measured at 550 nm.

2.7 Insulin Resistance Index

(1) Homeostasis model assessment of insulin resistance (HOMA-IR).

Systemic insulin resistance was estimated by HOMA-IR:

HOMA-IR = FBG (mmol/L) × Insulin (mIU/L) /22.5.

(2) Adipose tissue insulin resistance index (Adipo-IR).

Adipo-IR = FFA (mmol/L) × Insulin (µIU/L).

The Adipo-IR index has emerged as a predictive factor for metabolic syndrome-related diseases and effectively reflects the role of visceral adipose tissue in the development of insulin resistance [10,11].

2.8 Quantitative Real-Time PCR (RT-qPCR)

Total RNA was isolated from epididymal adipose tissue. Reverse transcription of the cDNA was completed with an All-in-one First Strand cDNA Synthesis Kit II (SM134, Saiwen Innovation Biotechnology Co., Ltd., Beijing, China). For reverse transcription-quantitative PCR (RT-qPCR), target gene primers were diluted 10-fold, and cDNA was diluted 5-fold. These were then mixed with SYBR Green qPCR MasterMix II (SM-143-01, Saiwen Innovation Biotechnology Co., Ltd., Beijing, China) in a final reaction volume of 20 µL. Table 1 lists all primer sequences used in this study. The $2^{-\Delta\Delta Ct}$ formula was employed to calculate gene expression levels.

2.9 Targeted Lipidomics Analysis

Targeted lipidomics analysis was performed using samples of murine epididymal adipose tissue. To monitor instrument stability and ensure data reproducibility, pooled quality control (QC) samples were prepared by mixing equal aliquots of all epididymal adipose tissue samples. These QC samples were injected periodically throughout the analytical run to monitor instrument stability. Data reproducibility was assessed by evaluating the relative standard deviation (RSD) of all detected lipids in the QC samples. Only lipids with RSD ≤30% were considered stable and retained for further analysis. Additionally, Pearson correlation coefficients between QC samples were all greater than 0.9, confirming the high repeatability of the measurements. To an appropriate amount of tissue sample, methanol (200 µL), an internal standard mixture (10 µL), and methyl tert-butyl ether (800 µL) were sequentially added, and samples were fully mixed. Samples were then vortexed, sonicated, placed in a cold water bath for 20 minutes, and allowed to stand at room temperature for 30 minutes. Next, 200 µL of mass spectrometry-grade water was added to each sample, followed by vortexing and centrifugation at 14,000 rpm at 4 °C for 15 minutes. The upper organic phase was collected and dried under a nitrogen stream. The dried extract was dissolved in 200 µL of a 90% isopropanol/acetonitrile solution, vortexed thoroughly, and centrifuged at 14,000 rpm at 4 °C for 15 minutes. The supernatant was used for subsequent analysis. Sample separation was performed using C18 (Torrance, CA, USA) and amino columns on the LC-30AD (Shimadzu Corporation, Kyoto, Japan) ultra-high-performance liquid chromatography system. The entire analytical process for samples was carried out with a 10 °C autosampler. Samples were analyzed continuously in a random order within the instrument to minimize signal fluctuations. Electrospray ionization (ESI) technology enables concurrent analysis of samples in both positive and negative ion modes. The samples were separated by ultra-high performance liquid chromatography (UHPLC), and mass spectrometry analysis was performed using an AB6500+QTRAP (ABSCIEX, Framingham, MA, USA) mass spectrometer. The above-mentioned targeted lipidomics analysis was performed by Shanghai Applied Protein Technology Co., Ltd.

Table 1. Primer sequences.

Primer	Primer sequences
Abhd2-Forward	5′-ACAGCCTTGTATGGGAAGATG-3′
Abhd2-Reverse	5′-TCGAAGAGGTCGAAGGTAGAA-3′
Acaca-Forward	5′-TCTCTGGTGGGATGAAAGATATGTA-3′
Acaca-Reverse	5′-ACCATTACAGGCTGGGAACAT-3′
Acadm-Forward	5′-GAGAAGAAGGGTGACGAGTATG-3′
Acadm-Reverse	5′-GGCTTTACTAGCGGGTACTTTA-3′
Adiponectin-Forward	5′-TGAGACAGGAGATGTTGGAATG-3′
Adiponectin-Reverse	5′-ACGCTGAGCGATACACATAAG-3′
Agpat2-Forward	5′-CAGAAGAAACTGGAGGTGGATG-3′
Agpat2-Reverse	5′-CACAGCGCTTAGGGAGTATTT-3′
Cd36-Forward	5′-CTGGGACCATTGGTGATGAAA-3′
Cd36-Reverse	5′-CACCACTCCAATCCCAAGTAAG-3′
Cept1-Forward	5′-CGGCTAGAAGAACACAGGTATC-3′
Cept1-Reverse	5′-CCAACTAGCCATTCCCAGTATC-3′
Cpt1a-Forward	5′-GAAGTGTCGGCAGACCTATTT-3′
Cpt1a-Reverse	5′-GTCCTCCTCTCTATATCCCTGTT-3′
Cpt2-Forward	5′-CCTGCATACCAGCGGATAAA-3′
Cpt2-Reverse	5′-CCTATCCAGTCATCGTGAACAG-3′
Dgat1-Forward	5′-GGCCTTACTGGTTGAGTCTATC-3′
Dgat1-Reverse	5′-GTTGACATCCCGGTAGGAATAA-3′
Etnk1-Forward	5′-GGGACTCTGGGCTTTGATAC-3′
Etnk1-Reverse	5′-CTGTGACCTCAGGCTTCATT-3′
Fabp4-Forward	5′-ATGGTGACAAGCTGGTGGAAT-3′
Fabp4-Reverse	5′-TCTTCCTTTGGCTCATGCCC-3′
Fasn-Forward	5′-TCCAGAGCCCAGACAGAGAA-3′
Fasn-Reverse	5′-CTGTGACCATGTCCACACCA-3′
Fdps-Forward	5′-TCGGGTGAAAGCACTGTATG-3′
Fdps-Reverse	5′-GCACTGCTCTATGAGACTCTTG-3′
Hadha-Forward	5′-GAGGAGGACTTGAGCTTGCC-3′
Hadha-Reverse	5′-AGCAACACTTCAGGGACACC-3′
Hmgcs1-Forward	5′-GCGTCTTTGCTTGTGTCTAATC-3′
Hmgcs1-Reverse	5′-GAGAACACTCCAACCCTCTTC-3′
IL-6-Forward	5′-CTTCCATCCAGTTGCCTTCT-3′
IL-6-Reverse	5′-CTCCGACTTGTGAAGTGGTATAG-3′
Leptin-Forward	5′-CCTGTGGCTTTGGTCCTATC-3′
Leptin-Reverse	5′-TGATGAGGGTTTTGGTGTCA-3′
Lipe-Forward	5′-CATCAACCACTGTGAGGGTAAG-3′
Lipe-Reverse	5′-AAGGGAGGTGAGATGGTAACT-3′
Lpcat1-Forward	5′-GAAGACAGTGGAGGAGATCAAG-3′
Lpcat1-Reverse	5′-GGTAATGAGGCAGGTCCTATTT-3′
Lpcat3-Forward	5′-TCGTGCTTCAGTTCCTCATC-3′
Lpcat3-Reverse	5′-CCGGTGGCTGTGATGTAATATC-3′
Pemt-Forward	5′-TGTGCTGTCCAGCTTCTATG-3′
Pemt-Reverse	5′-GAAGGGAAATGTGGTCACTCT-3′
Pnpla2-Forward	5′-TGCAGCACATTTATCCCGGT-3′
Pnpla2-Reverse	5′-CATCCACATAGCGCACCCC-3′
Ppargc1α-Forward	5′-CTAGCCATGGATGGCCTATTT-3′
Ppargc1α-Reverse	5′-GTCTCGACACGGAGAGTTAAAG-3′
Prdm16-Forward	5′-CACAAGTCCTACACGCAGTT-3′
Prdm16-Reverse	5′-TTGTTGAGGGAGGAGGTAGT-3′
Srebf1-Forward	5′-GGGCACTGAAGCAAAGCTGA-3′
Srebf1-Reverse	5′-TGCTGCAAGAAGCGGATGTA-3′

Table 1. Continued.

Primer	Primer sequences
TNF-α-Forward	5′-TTGTCTACTCCCAGGTTCTCT-3′
TNF-α-Reverse	5′-GAGGTTGACTTTCTCCTGGTATG-3′
Ucp-1-Forward	5′-GAGGTCGTGAACGTCAGAATG-3′
Ucp-1-Reverse	5′-AAGCTTTCCTGTGGTGGCTATAA-3′
β-actin-Forward	5′-GAGGTATCCTGACCCTGAAGTA-3′
β-actin-Reverse	5′-CACACGCAGCTCATTGTAGA-3′

IL-6, interleukin-6; TNF-α, tumor necrosis factor alpha.

2.10 Metabolic Pathway Analysis

The screening criteria for differentially abundant metabolites when comparing groups in the lipidomics dataset were as follows: variable importance in projection (VIP) >1, $p < 0.05$, and fold-change (FC) <0.5 or FC >1.2. Kyoto Encyclopedia of Genes and Genomes (KEGG) pathway analyses were used to explore metabolite enrichment. Principal Component Analysis (PCA) was completed in MetaboAnalyst (https://www.metaboanalyst.ca/).

2.11 Statistical Analysis

All data are presented as mean ± SEM. Graphs and corresponding statistical tests were performed using GraphPad Prism 10 (Version 10, San Diego, CA, USA). The Shapiro-Wilk test was used to assess the normality of these data, after which they were analyzed using paired *t*-tests or Mann-Whitney U tests, as appropriate. $p < 0.05$ was considered statistically significant.

3. Results

3.1 Semaglutide Improves the Systemic Metabolic Phenotype in Type 2 Diabetic Mice

To evaluate the systemic metabolic effects of semaglutide, a mouse model of T2DM was established using HFD combined with STZ administration. A subset of the resulting T2DM model mice was subsequently treated with semaglutide (HFS group). Fig. 1A (Ref. [12]) provides a schematic overview of the animal experimental workflow. As expected, after induction with HFD combined with STZ, the diabetic mice exhibited a progressive increase in food intake relative to pre-induction levels (Fig. 1C), significantly higher body weight than the control (CON) group (Fig. 1B), and fasting blood glucose levels >11.1 mmol/L (Fig. 1D), which are typical manifestations of T2DM. Administration of semaglutide (60 μg/kg/d, s.c. for 8 weeks) effectively attenuated the body weight gain in the HFS group compared to the HFD group. The HFD group showed significantly elevated blood glucose levels at 30, 60, 90, and 120 minutes during the IPGTT and by a substantially increased area under the curve (AUC), indicating severe impairment of glucose tolerance compared to the CON group. Compared to the HFD group, semaglutide treatment markedly improved glycemic control, as shown by a consistent downward trend in blood glucose levels and a significantly reduced AUC (Fig. 1D,E). In addition, fasting insulin levels in the HFD group were significantly increased compared to the HFS group. Calculation of the HOMA-IR insulin resistance index confirmed systemic insulin resistance in the HFS group, but the values were significantly decreased compared to those in the HFD group (Fig. 1F,G). In addition, we found that HFD/STZ induction elicited a dyslipidemic state, with increased TG, TC, and LDL-C levels compared to CON mice, along with decreased HDL-C levels. Treatment with semaglutide effectively counteracted this dyslipidemia and normalized serum lipid profiles compared with the HFD group (Fig. 1H). Collectively, our findings indicated that semaglutide confers systemic metabolic benefits in this T2DM mouse model and leads to significant improvements in body weight, glucose homeostasis, insulin sensitivity, and serum lipid profiles.

3.2 Semaglutide Improves Adipose Tissue Morphology and Alleviates Adipose Insulin Resistance

Next, we investigated the effect of semaglutide on the morphology of visceral adipose tissue and lipid-related metabolic parameters. Compared with the HFD group, the HFS group exhibited a striking reduction in the volume of epididymal white adipose tissue (eWAT) (Fig. 2A), suggesting a decrease in lipid storage. Moreover, both the absolute mass of white adipose tissue (WAT) and the WAT index (WAT-to-body weight ratio) were significantly reduced in the HFS group relative to the HFD group (Fig. 2B). In contrast, semaglutide treatment significantly increased brown adipose tissue (BAT) mass compared with the HFD group (Fig. 2C). Systemically, semaglutide markedly reduced serum levels of free fatty acids (FFAs) (Fig. 2D), indicating decreased lipolysis and/or enhanced fatty acid clearance. The adipose Adipo-IR index, calculated from fasting FFA and insulin levels, was also greatly ameliorated by semaglutide treatment (Fig. 2E). H&E staining further showed the amelioration of dysfunction in both BAT and WAT. Specifically, BAT in the semaglutide-treated mice regained its typical multilocular morphology with smaller lipid droplets as opposed to the unilocular morphology observed in the HFD group (Fig. 2F). We further examined the molecular levels of thermogenic genes and mitochondrial activation-related genes (*Ucp1*, *Ppargc1α*, *Prdm16*) in BAT (Fig. 2G). The results showed that, compared with

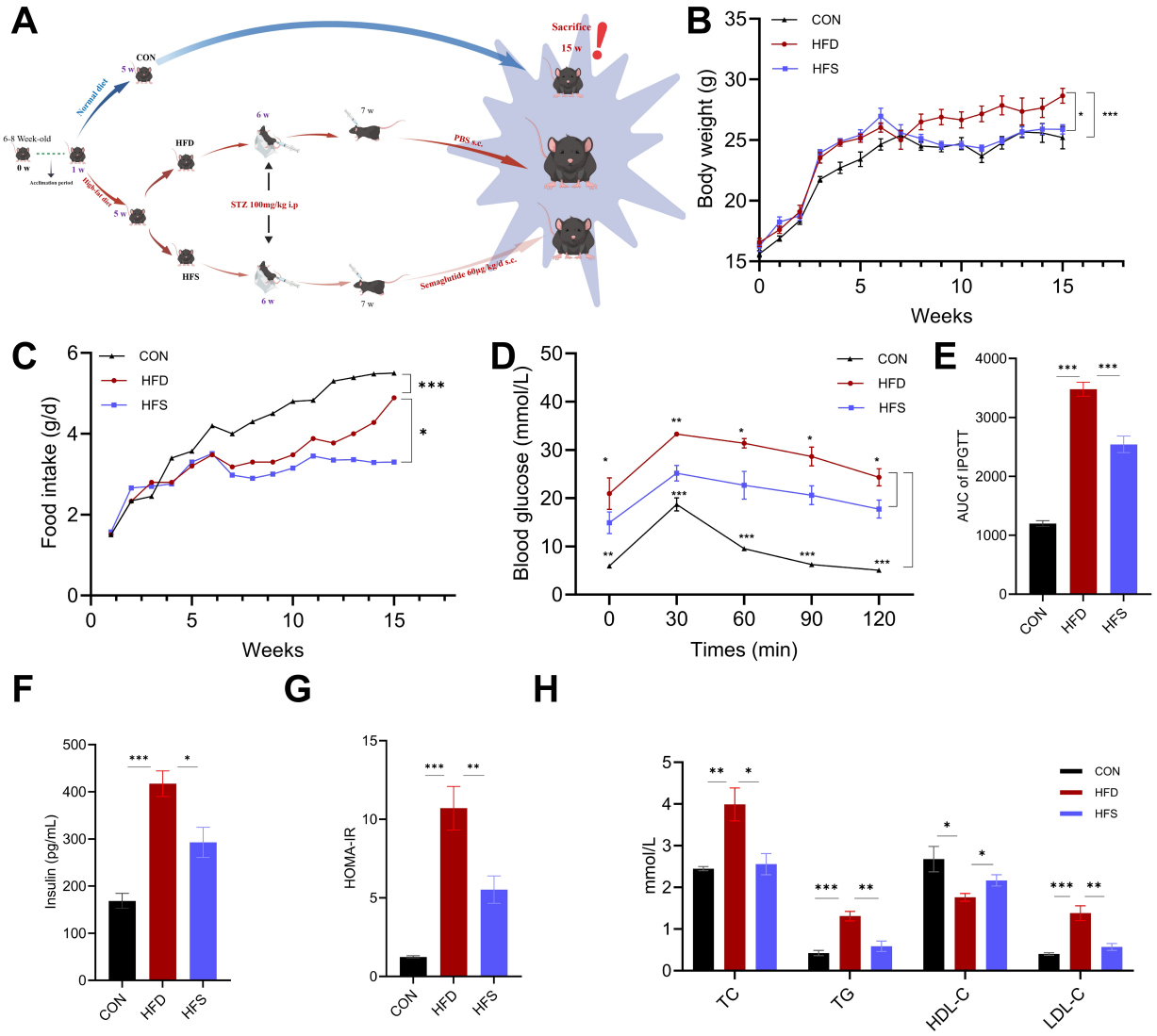

Fig. 1. Metabolic and biochemical parameters of mice under experimental conditions. (A) Schematic diagram of the experimental procedure (Fig. 1A was created with BioGDP.com [12]). (B) Changes in body weight of mice during the 15-week experiment. (C) Changes in food intake in the control (CON) group, high-fat diet (HFD) group and treated with semaglutide (HFS) group over the 15-week experimental period (D) Blood glucose levels during the intraperitoneal glucose tolerance test (IPGTT). (E) Area under the curve (AUC) for the IPGTT. (F) Serum fasting insulin levels. (G) Homeostatic model assessment of insulin resistance (HOMA-IR). (H) Serum levels of triglycerides (TG), total cholesterol (TC), lipoprotein high-density lipoprotein cholesterol (HDL-C), and low-density lipoprotein cholesterol (LDL-C) in CON, HFD, and HFS groups of mice. Data are expressed as mean ± SEM. n = 7, *$p < 0.05$, **$p < 0.01$, ***$p < 0.001$ vs. HFD group.

HFD/STZ-induced T2DM mice, the expression of these genes was significantly upregulated following semaglutide intervention. This demonstrates that semaglutide treatment activates brown adipose tissue and enhances its energy metabolism in T2DM mice. Moreover, H&E staining of eWAT (Fig. 2H) showed that the pronounced adipocyte hypertrophy evident in diabetic mice was markedly reduced by semaglutide treatment. This morphological improvement was supported by quantitative analysis, which showed a significant shift in adipocyte size distribution toward a greater proportion of smaller cells (Fig. 2I), consistent with the remodeling of VAT in these T2DM model mice.

3.3 Semaglutide Alleviates Hepatic Steatosis in Association With Improved Adipose Tissue Insulin Resistance

Evaluation of liver tissue samples from our experimental mice demonstrated that liver weight and liver index (liver-to-body weight ratio) values in the HFD group were markedly increased compared with the CON group, while these changes were reversed by semaglutide treatment (Fig.

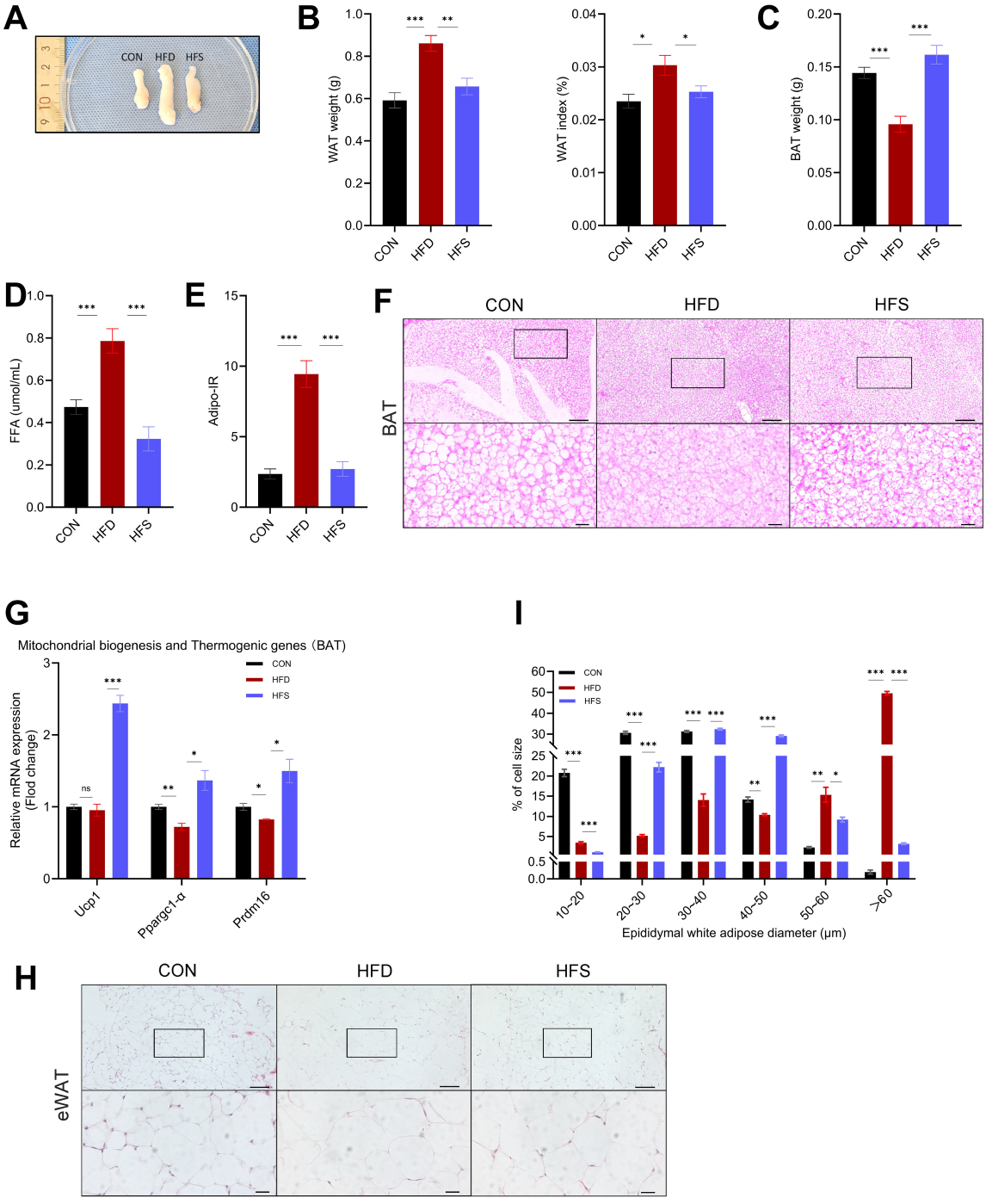

Fig. 2. Semaglutide improves adipose tissue morphology and alleviates adipose insulin resistance (Adipo-IR). (A) Representative images of epididymal white adipose tissue (eWAT). (B) Visceral White adipose tissue (WAT) mass (left panel) and WAT index (right panel), calculated as the WAT-to-body weight ratio. (C) Brown adipose tissue (BAT) mass. (D) Serum levels of free fatty acids (FFAs). (E) Adipose tissue insulin resistance (Adipo-IR) index. (F) Representative hematoxylin-eosin (H&E) stained sections of brown adipose tissue (BAT). Scale bars, 100 μm (main image) and 20 μm (inset). (G) mRNA expression levels of *Ucp1*, *Ppargc1α*, and *Prdm16* in BAT measured by reverse transcription-quantitative PCR (RT-qPCR). (H) Representative H&E stained sections of eWAT. The inset shows a higher-magnification view of the boxed area. Scale bars, 100 μm (main image) and 20 μm (inset). (I) Quantitative analysis of adipocyte size distribution in eWAT, presented as the percentage of adipocytes within each size range. Data are expressed as mean ± SEM. ns, not significant; *$p < 0.05$, **$p < 0.01$, ***$p < 0.001$ vs. HFD group.

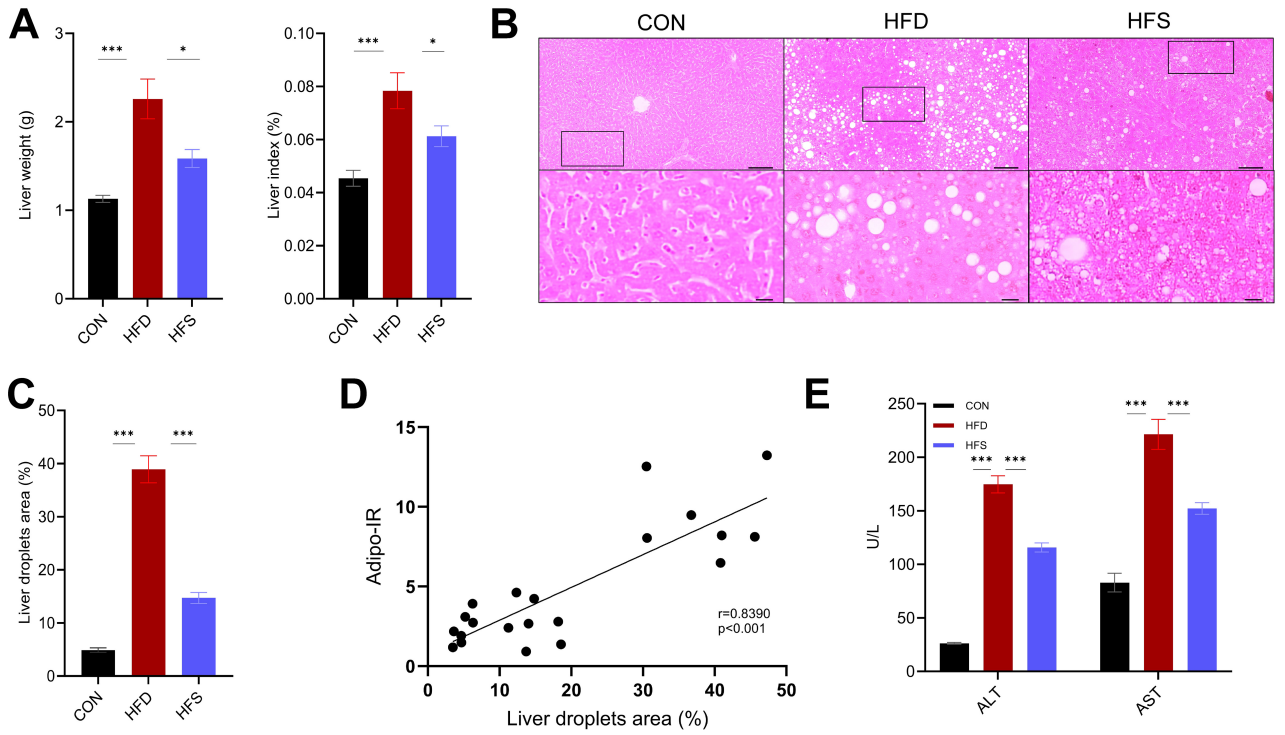

Fig. 3. Amelioration of hepatic steatosis by Semaglutide concurs with improved insulin sensitivity in adipose tissue. (A) Liver mass (left panel) and liver index (right panel), calculated as the liver-to-body weight ratio. (B) Representative H&E-stained sections of the liver. The inset shows a higher-magnification view of the boxed area. Scale bars, 100 μm (main image) and 20 μm (inset). (C) Quantitative analysis of hepatic lipid droplet area. (D) Correlation analysis between Adipo-IR and hepatic lipid droplet area (n = 7). The relationship was assessed by Pearson's correlation analysis. (E) Serum levels of aminotransferase (ALT), aspartate aminotransferase (AST). Data are expressed as mean ± SEM. *$p < 0.05$, ***$p < 0.001$ vs. HFD group.

3A). H&E staining showed further evidence of variably sized circular vacuoles within the livers of the HFD/STZ mice, consistent with hepatic steatosis (Fig. 3B). Quantitative analysis of H&E staining confirmed that semaglutide significantly decreased the area of lipids in the liver compared to the HFD group (Fig. 3C). Pearson correlation analysis indicated a significant positive relationship between the Adipo-IR index and the percentage of hepatic lipid droplet area (r = 0.8390, $p < 0.001$; Fig. 3D), which further suggested that the reduction in hepatic lipid accumulation induced by semaglutide is related to insulin resistance of adipose tissues. Compared to the CON group, serum ALT and AST levels increased significantly in the HFD group, whereas the liver function was significantly reduced in the HFS group (Fig. 3E). Collectively, these findings indicate that semaglutide ameliorates hepatic steatosis and liver injury by reducing adipose tissue insulin resistance.

3.4 Semaglutide Ameliorates Visceral Adipose Tissue Inflammation and Its Associated Systemic Inflammatory Profiles

We further investigated the effect of semaglutide on local and systemic inflammation in this mouse model of T2DM. Compared with the CON group, the HFD group had significantly increased serum Leptin levels (Fig. 4A). However, serum Adiponectin levels significantly increased after semaglutide treatment, indicating a shift toward an anti-inflammatory profile (Fig. 4B). Histological evaluation of VAT further supported the anti-inflammatory role of semaglutide. Systemically, semaglutide significantly reduced the serum levels of the inflammatory cytokines IL-6 and TNF-α, bringing their levels closer to those in the CON group (Fig. 4C). Immunohistochemistry (IHC) staining for F4/80 revealed that semaglutide reduced HFD-induced macrophage infiltration, and quantitative analysis confirmed a significant decrease in the proportion of macrophages in eWAT (Fig. 4D). We also evaluated inflammation in visceral WAT at the molecular level and found that *Leptin* mRNA levels were significantly upregulated in HFD/STZ and downregulated after semaglutide treatment, while *Adiponectin* mRNA levels were significantly upregulated after semaglutide treatment (Fig. 4E). Inhibition of *IL-6* and *TNF-α* expression by semaglutide was also confirmed in RT-qPCR analyses of visceral WAT (Fig. 4F). Taken together, these results demonstrate that semaglutide attenuates visceral adipose tissue inflammation and modulates systemic inflammatory responses in diabetic mice.

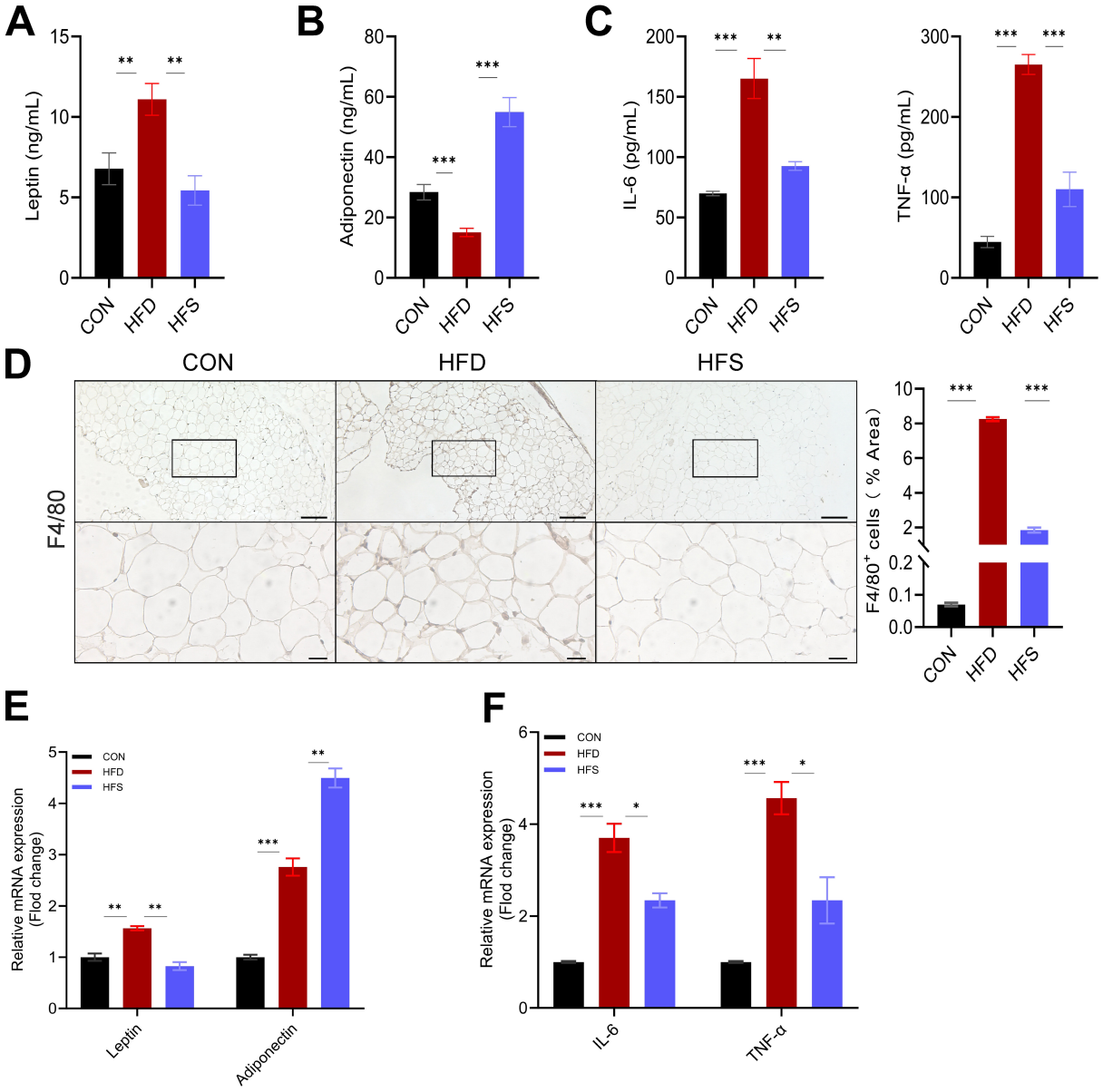

Fig. 4. Semaglutide suppresses macrophage infiltration into visceral adipose tissue and mitigates systemic inflammation. (A) Serum concentration of Leptin. (B) Serum concentration of Adiponectin. (C) Serum concentrations of IL-6 and TNF-α. (D) Macrophage infiltration in eWAT. Left panel: Representative immunohistochemical (IHC) staining for the macrophage marker F4/80 in eWAT. Scale bar, 100 μm (main image) and 20 μm (inset). Right panel: Quantitative analysis of F4/80-positive area. (E) mRNA expression levels of *Leptin* and *Adiponectin* in eWAT measured by RT-qPCR. (F) mRNA expression levels of *IL-6* and *TNF-α* in eWAT, as determined by RT-qPCR. Data are expressed as mean ± SEM. *$p < 0.05$, **$p < 0.01$, ***$p < 0.001$ vs. HFD group.

3.5 Semaglutide Remodels Lipid Metabolism in Visceral Adipose Tissue of Type 2 Diabetic Mice

To investigate changes in lipid composition within visceral WAT, we performed a targeted lipidomic analysis. A total of 1276 lipids were identified using this approach, including five major classes: glycerolipids (GL), glycerophospholipids (GP), fatty acids (FA), sterol lipids (ST), and sphingolipids (SP), which were further classified into 24 subclasses. Principal component analysis (PCA) of the resulting lipidomic profiles revealed clear separation among the CON, HFD, and HFS groups, reflecting distinct lipid metabolic states (Fig. 5A). Fig. 5B displays the number of lipid molecules identified within each lipid subclass. Comparative analysis of the HFD and HFS groups indicated that the levels of 50 lipids had significantly changed (VIP >1, $p < 0.05$, and FC >1.2 or <0.5). We first focused on glycerolipids due to their central roles in lipid storage and metabolic regulation in adipose tissue. Our targeted lipidomics data revealed that 9 TG species were significantly changed in visceral adipose tissue across

the experimental groups, including TG(55:2)-FA18:1, TG(56:2)-FA16:0, TG(56:3)-FA18:0, TG(56:3)-FA20:2, TG(56:9)-FA22:6, TG(58:10)-FA18:2, TG(58:10)-FA22:6, TG(58:9)-FA22:5, and TG(60:11)-FA22:6. It is worth noting that the HFD group showed a significant ~4-fold increase in TG(56:3)-FA20:2 levels compared with the CON group. However, TG(56:3)-FA20:2 levels were reduced by about half after semaglutide administration (Fig. 5C). Diacylglycerols (DG) serve as important signaling molecules and metabolic intermediates that can affect insulin sensitivity and lipid metabolism. Compared to the CON group, DG(18:1/18:2), DG(20:2/20:2), and DG(16:1/18:1) were significantly more abundant in the HFD group. Additionally, the levels of 11 DG species, including DG(18:1/18:2), DG(18:2/18:2), DG(18:3/20:0), DG(20:2/20:2), DG(15:0/20:2), DG(16:1/18:1), DG(16:1/18:2), DG(16:1/20:1), DG(16:1/20:2), DG(16:1/20:3), and DG(16:1/22:4) declined significantly after semaglutide treatment (Fig. 5D). The total fatty acid content of adipose tissue from HFD/STZ-induced diabetic mice did not differ significantly compared to the CON group, whereas semaglutide treatment resulted in a marked decrease in fatty acid levels relative to the HFD group (Fig. 5E). Moreover, levels of the ChE(22:1) were elevated in the HFD group compared to the CON group, while ChE(22:1) content was restored to near-normal levels after semaglutide treatment (Fig. 5F). We also performed hierarchical clustering of the significantly altered glycerophospholipid species identified in this study. In the resulting heatmap, distinct separation was evident between the HFD and HFS groups, revealing that semaglutide induced substantial remodeling of multiple glycerophospholipid species, including glycerophosphocholines (PC), glycerophosphoethanolamines (PE), plasmalogen PE (PE-P), glycerophosphoglycerols (PG), glycerophosphoserines (PS), lyso-glycerophosphocholines (LPC), and lyso-glycerophosphoinositols (LPI) (Fig. 5G). Lipid pathway enrichment analysis (LIPEA) of the altered lipids revealed that the majority of the top 15 enriched pathways were associated with lipid metabolism, with glycerophospholipid metabolism being the most significantly enriched. Key lipid-related pathways also identified using this approach included fat digestion and absorption, cholesterol metabolism, regulation of lipolysis in adipocytes, fatty acid biosynthesis, and thermogenesis. Furthermore, significant enrichment of pathways including "lipid and atherosclerosis" and "insulin resistance" was also observed, emphasizing the critical link between the observed lipidomic alterations and the pathophysiological features of T2DM and associated complications (Fig. 5H). Collectively, our lipidomic analysis reveals that the metabolic benefits of semaglutide are associated with the concerted restructuring of glycerolipid and glycerophospholipid metabolism in VAT.

3.6 Semaglutide Modulates the Expression of Lipid Metabolism Genes in Visceral Adipose Tissue and Its Systemic Correlations

Based on our LIPEA results pertaining to lipid metabolism pathways in adipose tissue, we performed RT-qPCR analyses of key regulatory genes within the significantly enriched pathways in VAT to help better characterize the mechanisms underlying semaglutide-induced lipid metabolic remodeling. This approach included validating upstream and downstream genes involved in lipogenesis and lipolysis, glycerolipid/glycerophospholipid metabolism, cholesterol metabolism, and fatty acid β-oxidation and transport. As shown in Fig. 6A–F, RT-qPCR results demonstrated that semaglutide significantly modulated the mRNA levels of critical enzymes and regulators involved in multiple lipid metabolic pathways in eWAT tissue samples compared to the CON group. In the lipolysis pathway (Fig. 6A), the mRNA levels of *Lipe* and *Pnpla2* were significantly downregulated in the HFD group compared to the CON group, but were significantly upregulated by semaglutide treatment. In contrast, lipogenic genes (*Acaca*, *Fasn*; Fig. 6B) were markedly induced in the HFD group, and this effect was abolished by semaglutide administration. Among genes involved in glycerolipid and glycerophospholipid metabolism, *Lpcat1*, *Lpcat3*, *Etnk1*, and *Agpat2* were significantly upregulated in the HFD group and downregulated by semaglutide (Fig. 6C). Conversely, *Abhd2* expression was suppressed in the HFD group but was significantly restored by semaglutide administration. In addition, *Pemt* and *Cept1* levels showed a significant increasing trend in the HFD group, but were significantly suppressed after semaglutide administration. Genes related to fatty acid oxidation (*Acadm*, *Cpt1a*, *Cpt2*, *Hadha*; Fig. 6D) were not significantly affected by HFD/STZ induction, whereas semaglutide robustly enhanced their expression. Similarly, the expression of fatty acid transport genes was significantly modulated by semaglutide. In contrast, *Cd36* and *Fabp4* expression was markedly increased in the HFD group compared to the CON group, but significantly decreased after semaglutide treatment (Fig. 6E). Genes related to cholesterol metabolism (*Srebf1*, *Hmgcs1*, and *Fdps*) were significantly up-regulated in the HFD group, and semaglutide effectively reversed their expression (Fig. 6F). Additionally, we examined the expression of key browning-related genes in epididymal adipose tissue. Compared with the HFD group, HFS group significantly upregulated the mRNA levels of uncoupling protein 1 (*Ucp1*), peroxisome proliferator-activated receptor gamma coactivator 1-alpha (*Ppargc1α*), and PR domain containing 16 (*Prdm16*) in eWAT (Fig. 6G). This coordinated upregulation suggests a role in promoting mitochondrial uncoupling thermogenesis, enhancing mitochondrial biogenesis, and driving browning in WAT.

Pearson correlation analysis was conducted to examine the association between lipid species in visceral

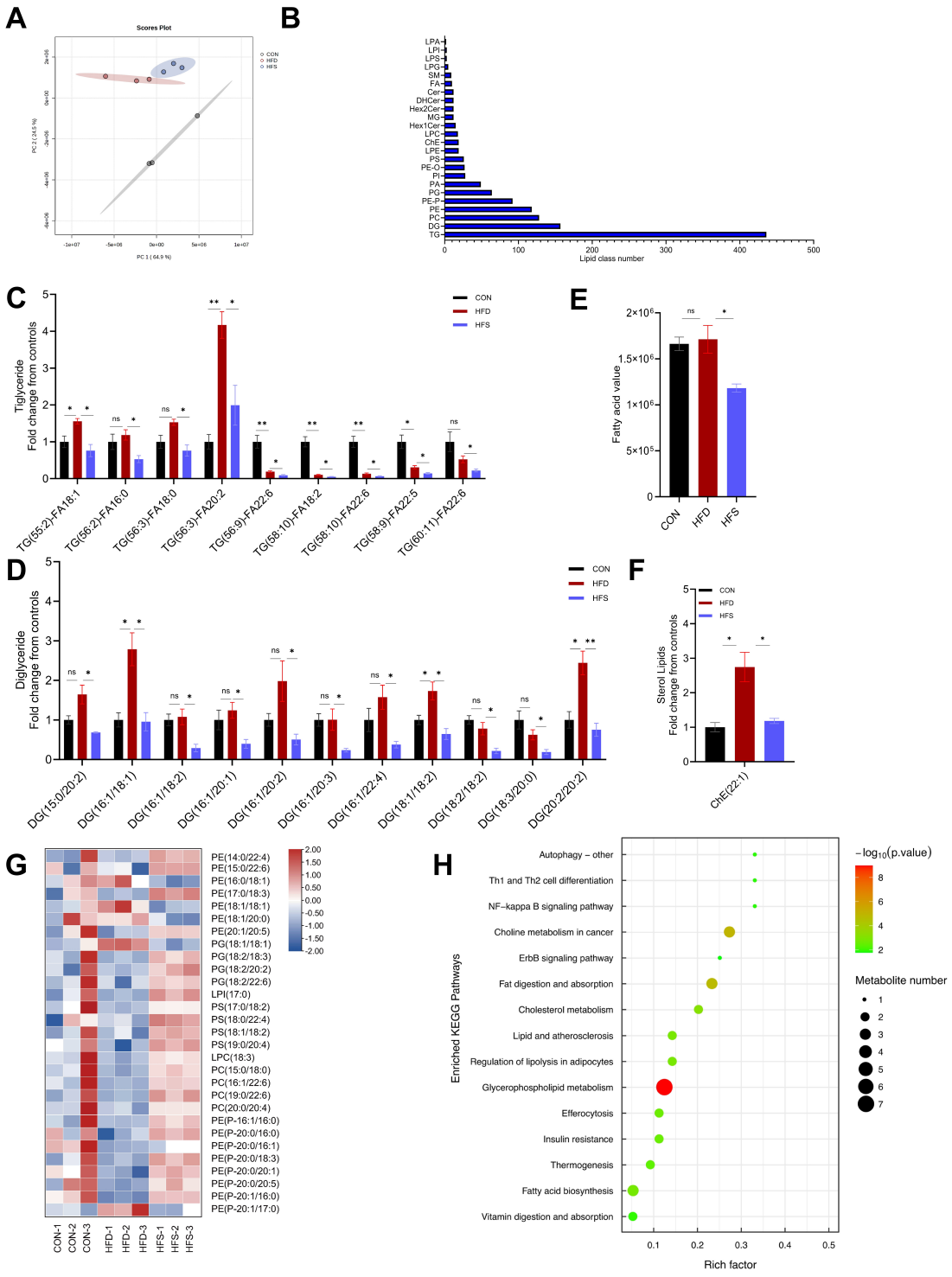

Fig. 5. Comparative lipidomic analysis of visceral adipose tissues in CON, HFD, and HFS groups. (A) Principal component analysis (PCA) score plot. (B) The number of identified lipid species within each lipid class. (C–F) Relative abundance of significantly altered lipid species between groups for (C) triacylglycerols (TG), (D) diacylglycerols (DG), (E) fatty acid (FA), and (F) cholesteryl ester (ChE). Criteria: VIP >1, p-value < 0.05, and fold change >1.2 or <0.5. Data are presented as mean ± SEM. (n = 3 per group). (G) Heatmap of significantly altered glycerophospholipids (GP), filtered by the same significance criteria. (H) Lipid Pathway Enrichment Analysis (LIPEA) indicating enriched pathways in the Kyoto Encyclopedia of Genes and Genomes (KEGG) database. ns, not significant; *p < 0.05, **p < 0.01 vs. HFD group.

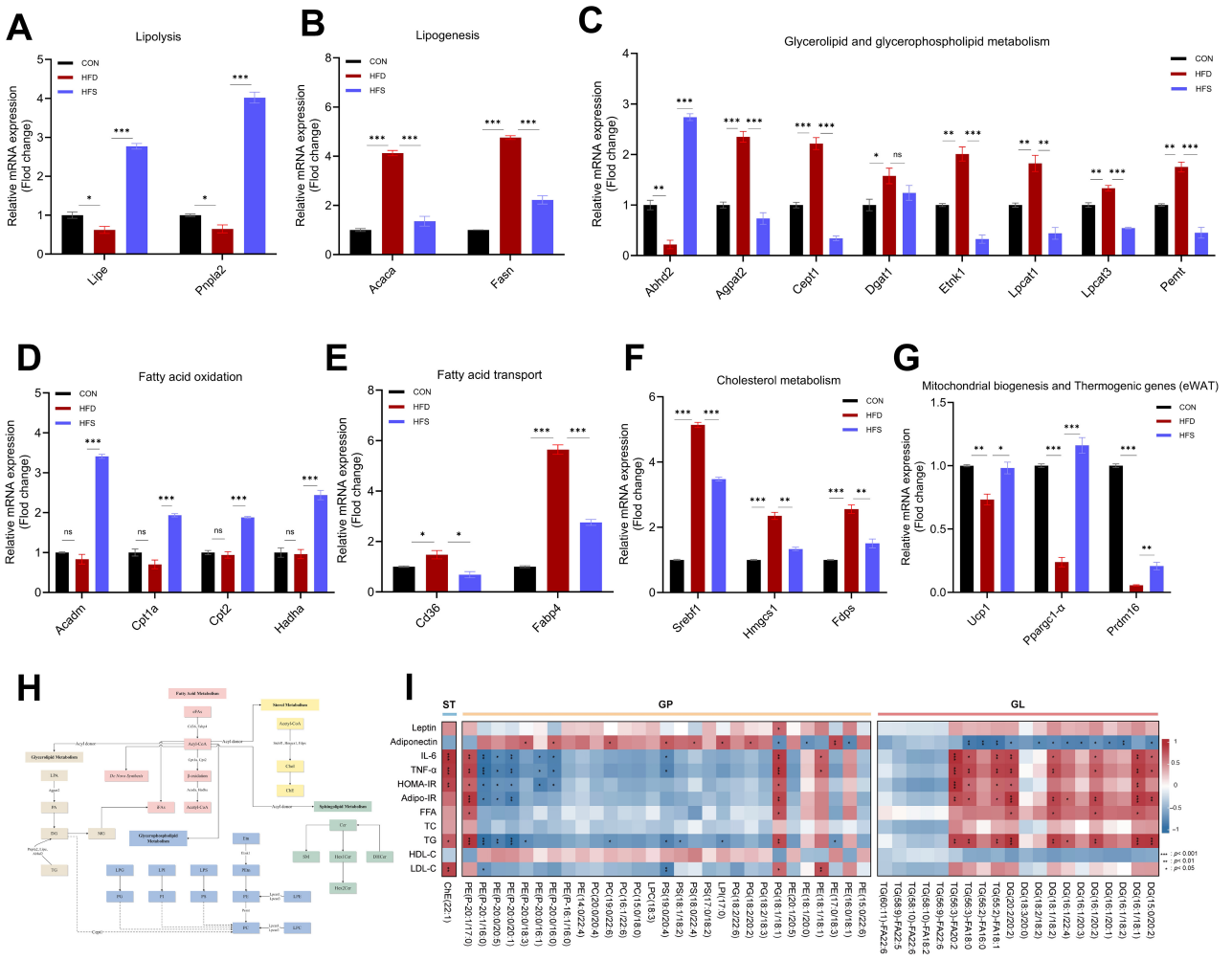

Fig. 6. Semaglutide coordinates visceral adipose tissue lipid metabolism by modulating gene expression and remodeling the lipidome. (A–G) mRNA expression levels of key genes involved in (A) lipolysis, (B) lipogenesis, (C) glycerolipid and glycerophospholipid metabolism, (D) fatty acid oxidation, (E) fatty acid transport, (F) cholesterol metabolism, and (G) mitochondrial biogenesis and thermogenic genes in eWAT, as determined by RT-qPCR. Data are presented as mean ± SEM. (H) Schematic diagram summarizing the proposed mechanism of semaglutide on adipose tissue lipidome remodeling through its effect on the expression of key lipid metabolic genes. (I) Pearson correlation analysis between significantly altered lipid metabolites and key biochemical indicators of metabolism and inflammation. Red and blue indicate positive and negative correlations, respectively. ns, not significant; *$p < 0.05$, **$p < 0.01$, ***$p < 0.001$ vs. HFD group.

WAT samples and various metabolic parameters significantly affected by semaglutide treatment, including inflammatory factors, adipokines, insulin resistance indices, and serum lipid profiles. DG(16:1/20:2), DG(16:1/18:1), DG(15:0/20:2), DG(20:2/20:2), DG(18:1/18:2), TG(56:3)-FA20:2, TG(56:3)-FA18:0, TG(55:2)-FA18:1, PG(18:1/18:1), and PE(P-20:1/17:0) levels showed strong positive correlations with IL-6 and TNF-α, as well as with Adipo-IR. Several specific DG and TG species in visceral adipose tissues, including TG(56:3)-FA18:0, TG(56:2)-FA16:0, TG(55:2)-FA18:1, DG(20:2/20:2), DG(18:2/18:2), DG(18:1/18:2), DG(16:1/22:4), DG(16:1/20:3), DG(16:1/20:2), DG(16:1/20:1), DG(16:1/18:2), and DG(15:0/20:2), were negatively correlated with levels Adiponectin, supporting the involvement of these DG and TG species in the impaired lipid metabolism that characterized T2DM. However, another distinct set of glycerophospholipids, including PE(P-20:0/16:0), PE(P-20:0/16:1), PE(P-20:1/16:0), PE(P-20:0/20:5), PE(P-20:0/20:1), and PS(19:0/20:4), displayed significantly negative correlations with IL-6 and TNF-α levels. PG(18:1/18:1) abundance was positively correlated with Leptin levels and negatively correlated with those of Adiponectin, highlighting its involvement in metabolic and inflammatory pathways (Fig. 6I). Semaglutide downregulated genes involved in lipogenesis and glycerolipid/glycerophospholipid metabolism, while upregulating those related to fatty acid oxidation , thus

lowering lipid accumulation and preserving metabolic balance. This schematic illustrates the mechanism by which semaglutide remodels the visceral adipose tissue lipid metabolism through integrating lipidomic and targeted gene expression data (Fig. 6H).

4. Discussion

The global incidence of T2DM is constantly increasing, constituting a significant public health challenge. The fundamental cause of this disease is the pathophysiological defects of insulin resistance and pancreatic β-cell dysfunction. A well-established animal model in which a high-fat diet is used to induce insulin resistance, followed by combined STZ injection, simulates the characteristics of T2DM, which is mainly characterized by insulin resistance accompanied by relative insulin deficiency. This method differs from high-dose STZ injection alone, which destroys pancreatic β-cells and induces absolute insulin deficiency typical of type 1 diabetes. Critically, dysfunction of VAT and its associated abnormal lipid accumulation further aggravate insulin resistance and β-cell dysfunction, thereby promoting the development of the disease [13,14,15]. Despite the well-recognized role of VAT in type 2 diabetic pathogenesis, the specific effects of GLP-1RA semaglutide on the lipid composition and remodeling of VAT in a type 2 diabetic context have not been elucidated. Here, we show that, beyond promoting weight loss and improving glucose homeostasis, semaglutide induces a multifaceted reorganization of the VAT lipidome. This reorganization is supported by coordinated changes in the expression of key lipid metabolic genes and is associated with significant improvements in insulin resistance and inflammation.

Semaglutide is a GLP-1RA exhibiting 94% amino acid sequence homology with human GLP-1 [16] that was approved by the U.S. Food and Drug Administration for the treatment of obesity in 2021. GLP-1R is broadly expressed in the central nervous system and peripheral tissues, including the pancreas, gastrointestinal tract, heart, kidney, and adipose tissue [17]. Nevertheless, the extrapancreatic mechanisms of GLP-1, particularly its role in adipose tissue, are still not fully understood. Rodríguez Jiménez et al. [18] demonstrated that in obese patients with T2DM, whether administered via subcutaneous injection or orally, semaglutide led to marked fat-related changes after 24 weeks, with respective decreases of 9.5% ± 5.7% and 9.4% ± 5.9% in body weight, and 30.2 cm^2 and 42.3 cm^2 in visceral fat area. The incidence of dyslipidemia in T2DM is estimated to range from 43.84% to 75.5%, and, according to epidemiological studies, controlling related risk factors can reduce the incidence of cardiovascular events by more than 50% [19,20,21] in affected patient populations. In this study, semaglutide effectively lowered the abnormally elevated levels of LDL-C, TG, and TC in our model mice, as previously reported [22,23,24]. Notably, semaglutide's effects on body weight, visceral fat, and lipids in T2DM were not confined to its effects on the pancreas. In the context of obesity and T2DM, the breakdown of adipose tissue is deregulated such that more fatty acids are released into circulation [25]. As a key metabolic hub, the liver takes up excess FFAs and re-esterifies them into TG, ultimately leading to excessive hepatic TG deposition [26]. We observed an increase in liver and WAT weight in our T2DM mouse model, accompanied by histological evidence of marked hepatic steatosis. Consistent with previous clinical evidence indicating that enlarged visceral adipocytes are associated with an 80% higher risk of insulin resistance per standard deviation increase in visceral adipose tissue volume, semaglutide effectively reversed these pathological changes [27]. Specifically, it reduced the proportion of hepatic lipid droplet area and decreased the size of hypertrophic WAT. Furthermore, Adipo-IR is well established as one of the main drivers of hepatic lipid accumulation and metabolic disorders [28]. We discovered a strong positive association between Adipo-IR values and the number of fat droplets in the livers of diabetic mice. These results together suggest that semaglutide may be able to reduce hepatic lipid accumulation predominantly through its ability to improve insulin resistance in adipose tissue.

In this study, the reduction in food intake was a significant factor contributing to the body weight loss and improvement in adipose tissue accumulation induced by semaglutide. Semaglutide suppresses appetite and reduces food intake by targeting central regions, such as the arcuate nucleus of the hypothalamus and the brainstem area postrema [23]. However, accumulating evidence suggests that its effects on adipose tissue are not solely dependent on appetite suppression. Teixidor-Deulofeu et al. [29] found that semaglutide can act on neurons expressing adenylate cyclase-activating polypeptide 1 in the dorsal vagal complex to directly promote fat breakdown and utilization, independent of food intake reduction. Byun et al. [30] demonstrated that the semaglutide-treated group exhibited unique adipose tissue remodeling effects by pair-feeding experiments, including a significant reduction in adipose tissue mass, enhanced browning of white adipose tissue, and increased sympathetic innervation in brown adipose tissue. These effects had not been observed in the caloric restriction-only group. Furthermore, *in vitro* studies had revealed the independent regulatory effects of GLP-1RAs on adipocytes. Mature preadipocytes treated with GLP-1 showed significant size reduction and an increase in the number of small-diameter adipocytes [31]. In summary, semaglutide exerts direct and independent pharmacological effects on adipocytes. Our results demonstrated that although semaglutide induced significant fat loss, some glycerophospholipids, such as glycerophosphocholines, glycerophosphoethanolamines, glycerophosphoglycerols, and glycerophosphoserines, were elevated. These changes were positively correlated with improvements in insulin resistance and reduced adipose tissue inflammation, indicat-

ing that the extent of lipidomic alterations did not parallel the degree of fat weight decrease induced by reduced food intake. This dissociation strongly suggests that the observed lipid remodeling cannot be solely attributed to reduced caloric intake. Pair-feeding experiments would be a valuable approach to definitively dissect the direct effects of semaglutide on adipose tissue independent of food restriction, and we considered such studies in our future work to further investigate the independent effects of semaglutide on adipose tissues.

The development of insulin resistance is associated with chronic adipocyte inflammation [32,33]. Under pathological conditions, visceral white adipocytes enlarge, while the intercellular density becomes sparse. This congestion causes hypoxia, which activates p38 phosphorylation and induces a state of inflammation in adipocytes [34,35]. Macrophage infiltration into adipose tissue is associated with both local and systemic inflammation, while GLP-1RAs have been shown to reduce local or systemic inflammation in T2DM or obesity in animals and patients [36,37,38]. Histological examination performed in the present study revealed positive F4/80 IHC staining in the eWAT of our HFD/STZ mice, indicating a high level of macrophage infiltration. Previously, studies have shown that M1 macrophages have been reported to induce adipocyte secretion of pro-inflammatory factors such as IL-6 and TNF-α [39], which supports our finding that serum levels of these cytokines, as well as their expression at the mRNA level in adipose tissue, were elevated in diabetic mice. Importantly, semaglutide significantly reduced macrophage accumulation and the release of inflammatory cytokines in visceral WAT. This finding is consistent with previous studies showing that GLP-1RAs can directly prevent pro-inflammatory signaling in macrophages and adipocytes, reducing the expression and release of key cytokines, including IL-6 and TNF-α [40,41]. Moreover, adipokines are major regulators of adipocyte inflammation. Leptin is recognized as pro-inflammatory and leads to the polarization of macrophages toward an M1 phenotype [42]. Conversely, adiponectin displays anti-inflammatory properties, supporting M2 macrophage polarization. The M1-to-M2 shift in the polarization of macrophages decreases adipose tissue inflammation and indirectly improves insulin resistance [43,44]. We found that the administration of semaglutide reversed Leptin resistance and increased Adiponectin expression in our T2DM model mice. In summary, semaglutide alleviates adipose tissue metabolic dysfunction by regulating key adipokines Leptin and Adiponectin, reducing IL-6- and TNF-α-mediated inflammation, and thereby halting the vicious cycle of insulin resistance and inflammation to preserve appropriate metabolic homeostasis.

High levels of insulin can directly inhibit HSL activity, which is encoded by the *Lipe* gene, in addition to indirectly impairing the localization and function of ATGL on lipid droplets that are encoded by the *Pnpla2* gene, ultimately leading to impaired lipolysis, lipid droplet inertia, and lipid metabolism dysfunction in type 2 diabetes. Conversely, increased *Fasn* and *Acaca* transcript levels promote lipid synthesis and accelerate the formation and accumulation of fatty acids and triglycerides [45,46]. This study has highlighted semaglutide's ability to correct this imbalance by suppressing lipogenic gene expression and upregulating lipolytic gene expression in type 2 diabetes. Triglycerides (TGs) are the most abundant lipids in WAT and serve as the major storage form of fatty acids. TG composition directly reflects the lipid storage status and functional properties of tissues. Herrera-Marcos et al. [47] reported that in a porcine nonalcoholic steatohepatitis (NASH) model, supplementation with squalene led to TG(55:2) becoming an important lipidomic change of improved hepatic steatosis. After treatment with Zuogui Jiangtang Qinggan Formula in NASH db/db mice, TG(56:3) levels in the liver were decreased compared with the model group [48]. In this study, both TG(55:2) and TG(56:3) were reduced in visceral WAT after semaglutide administration. The consistent downregulation of these specific TG species in various metabolic tissues and animal models indicates that TG(55:2) and TG(56:3) may be key conserved lipid metabolites associated with dysfunctional lipid metabolism. *Agpat2* play roles in TG synthesis, and studies by Pei et al. [49] confirmed *Agpat2* was significantly activated during adipocyte differentiation. Our findings demonstrated that semaglutide significantly suppressed the expression of *Agpat2* mRNAs, accompanied by reductions in TG(55:2) and TG(56:3) levels. Collectively, the changes in adipose tissue TG profiles induced by semaglutide are suggestive of an alleviation of lipid dysfunction in T2DM. Diacylglycerols (DGs) are essential secondary messengers that participate in different metabolic processes, regulating membrane dynamics and cellular signal transduction in mammals [50]. Masenga et al. [51] showed that DGs impair insulin signaling transduction by activating protein kinase C (PKC), while Szendroedi et al. [52] reported DG involvement in the pathogenesis of lipid-induced muscle insulin resistance through PKCθ in obese and T2DM. In our study, semaglutide significantly decreased DG(18:2/18:2) and DG(18:1/18:2) in the visceral WAT of mice. Importantly, DG(18:1/18:2) showed a strong correlation with Adipo-IR. The results not only confirm the significance of particular DGs across different forms of metabolism in different types of animals and interventions, but also show that semaglutide helps improve adipose tissue insulin sensitivity by regulating these specific DGs.

Glycerophospholipids are the main parts of cell membranes and participate in cellular signal transduction, and their remodeling is closely related to insulin sensitivity. Veen et al. [53] reported that phosphatidylcholine (PC) biosynthesis occurs primarily via the Pemt-mediated phosphatidylethanolamine (PE) methylation pathway and the

Cept1-mediated Kennedy pathway. Knocking out either *Pemt* or *Cept1* can decrease PC content, increase energy expenditure, and improve insulin sensitivity. Also, deleting *Lpcat3* in the livers of ob/ob and high-fat diet mouse models would reduce the abundance of PCs and lipogenesis, decrease membrane flexibility, and alleviate insulin resistance [54]. It was shown that semaglutide markedly downregulated the expression of *Lpcat3*, *Pemt*, and *Cept1* mRNAs in adipocytes. These findings indicate that semaglutide improves glycerophospholipid remodeling by regulating the transcription of key genes in adipose tissues of the T2DM model. Additionally, our results showed that PG(18:1/18:1) was positively correlated with IL-6, TNF-α, HOMA-IR, Adipo-IR, and Leptin, but negatively correlated with Adiponectin. Guo et al. [55] reported that glycerophospholipid metabolism was associated with in-hospital mortality and heart failure (HF) after acute myocardial infarction (AMI), and that PG(18:1/18:1) could serve as a potential biomarker for predicting the prognosis of AMI patients. AMI is accompanied by severe inflammation. Kayser et al. [56] showed that glycerophosphoglycerols (PG) were linked with inflammation and involved in adipose tissue remodeling in obesity. Therefore, these independent findings imply that PG(18:1/18:1) has adverse prognostic effects on systemic metabolic inflammation and insulin resistance. This directly supports the "common ground" hypothesis, which identifies specific lipid mediators that clarify the common pathophysiology between T2DM, obesity, and adverse cardiovascular events.

Moreover, our results found that ChE(22:1) is an abnormal metabolomic change specifically in diabetic fat tissue, and semaglutide can reverse this abnormal accumulation. We showed that *Srebf1* (a major regulatory gene for cholesterol and fatty acid synthesis), HMG-CoA synthase 1 (*Hmgcs1*, the initial limiting enzyme of cholesterol synthesis), Farnesyl diphosphate synthase (*Fdps*, a crucial enzyme in the production of cholesterol) mRNA expression promote the increase of free cholesterol pool in adipose tissue to offer providing an abundant of substrate for the abnormal esterification synthesis of ChE(22:1). Our observation showed ChE(22:1) was significantly positively correlated with IL-6, TNF-α, HOMA-IR, and lipid profiles (TG, LDL-C); however, no significant association was found with Adipo-IR. This correlation suggests that ChE(22:1) accumulation primarily reflects systemic rather than localized adipose tissue dysfunction. Additionally, semaglutide's effect on reducing ChE(22:1) may arise from its inhibition of *de novo* cholesterol synthesis at the transcriptional level by blocking the activation of key cholesterol synthesis genes, such as *Srebf1*, *Hmgcs1*, and *Fdp*s. These changes not only reduce the supply of free cholesterol at its source and the storage of ChE(22:1), but also extend the significance of ChE(22:1) beyond its traditional function as a sterol lipid in specific tissues [57,58].

Besides, the lipidomic analysis showed that although semaglutide significantly decreased the total fatty acid contents in the visceral WAT of the diabetic mice, no specific fatty acids significantly changed in abundance. Therefore, we hypothesize that semaglutide induces a non-selective, global pattern of fatty acid utilization in visceral WAT. After semaglutide treatment, adipose tissue lipolysis was enhanced, and released fatty acids were effectively directed toward mitochondrial β-oxidation for consumption. We found that semaglutide simultaneously reduces exogenous fatty acid uptake through suppressing fatty acid transporter genes (*Cd36*, *Fabp4*), while significantly upregulating key β-oxidation genes (*Acadm*, *Cpt1a*, *Cpt2*, *Hadha*) to enhance the catabolism of lipolytic products. This inference is further supported by markedly reduced circulating free fatty acid levels, suggesting enhanced "trapping" and utilization of fatty acids by adipose tissue [59,60].

In the present study, semaglutide intervention significantly upregulated the expression of *Ucp1*, *Ppargc1α*, and *Prdm16* in both eWAT and interscapular BAT. As representative markers of adipocyte thermogenic genes and mitochondrial activation genes, the increased expression of these genes directly reflects enhanced energy metabolism in adipose tissue. This finding is consistent with the morphological activation features we observed in brown adipose tissue. Research on WAT showed that GLP-1 receptor agonists activate the AMPK-SIRT1-PGC1α signaling, upregulate browning-related gene expression, and promote brown remodelling [61,62]. Furthermore, semaglutide treatment significantly upregulated *Cpt1a* gene expression in epididymal adipose tissue. The elevated expression of this gene enhances the rate-limiting step of mitochondrial fatty acid oxidation, directly driving energy metabolism and providing the energy substrate necessary for white adipose tissue browning, thereby supporting its transition toward a thermogenic phenotype [63,64]. The metabolic remodeling of visceral white adipose tissue and the functional activation of brown adipose tissue establish a synergistic lipid-processing system that effectively boosts the body's overall lipid turnover capacity. In summary, semaglutide induces a holistic, proportionate process of lipid mobilization and consumption, which leads to effective adipose tissue reduction while maintaining relative stability in intracellular fatty acid composition.

5. Study Limitations

Several limitations of this study should be acknowledged. The sample size for the targeted lipidomics analysis of epididymal white adipose tissue was limited to three per group, which meets only the minimum requirement for statistical analysis. This small sample size may limit the statistical power and generalizability of the findings, and future studies with larger cohorts are warranted to validate these results. Additionally, due to the absence of pair-fed control groups, we cannot definitively distinguish whether the

observed remodeling effects on visceral adipose tissue are direct consequences of semaglutide treatment or secondary to its systemic metabolic improvements. Future studies incorporating pair-feeding designs are necessary to elucidate the direct, adipose tissue-specific effects of semaglutide independent of its systemic actions.

6. Conclusions

In summary, this study demonstrates that semaglutide effectively improves lipid metabolism disorders in visceral white adipose tissue of type 2 diabetic mice. Its intervention not only reduces body weight, lowers blood glucose, and improves insulin resistance, but also profoundly remodels adipose tissue, specifically by decreasing adipocyte hypertrophy and macrophage infiltration. Targeted lipidomics and gene expression analyses further revealed that semaglutide broadly modulates metabolic pathways involving triglycerides, glycerophospholipids, fatty acids, and cholesterol, with the most pronounced reprogramming occurring in glycerophospholipid metabolism. Notably, this study mapped lipid molecular changes in epididymal white adipose tissue under semaglutide intervention, confirming its therapeutic effects through synergistic regulation across multiple lipid categories and metabolic pathways. This provides direct evidence for understanding the lipid molecular basis by which GLP-1 receptor agonists improve metabolic diseases.

Abbreviations

Abhd2, Abhydrolase domain containing 2; *Acaca*, Acetyl-Coenzyme A carboxylase alpha; *Acadm*, Acyl-Coenzyme A dehydrogenase, medium chain; Adipo-IR, Adipose tissue insulin resistance index; *Agpat2*, 1-acylglycerol-3-phosphate O-acyltransferase 2; ALT, Alanine aminotransferase; ATGL, Adipose triglyceride lipase; AUC, Area under the curve; BAT, Brown adipose tissue; *Cd36*, Cd36 molecule; *Cept1*, Choline/ethanolaminephosphotransferase 1; *Cpt1a*, Carnitine palmitoyltransferase-1a; *Cpt2*, Carnitine palmitoyltransferase 2; *Dgat1*, Diacylglycerol O-acyltransferase 1; eWAT, Epididymal white adipose tissue; *Etnk1*, Ethanolamine kinase 1; *Fasn*, Fatty acid synthase; *Fabp4*, Fatty acid binding protein 4; *Fdps*, Farnesyl diphosphate synthetase; FDA, Food and Drug Administration; FFA, Free fatty acids; GLP-1RAs, Glucagon-like peptide-1 receptor agonists; *Hadha*, Hydroxyacyl-CoA dehydrogenase trifunctional multienzyme complex subunit alpha; HDL-C, High-density lipoprotein Cholesterol; *Hmgcs1*, 3-hydroxy-3-methylglutaryl-Coenzyme A synthase 1; HOMA-IR, Homeostasis model assessment of insulin resistance; HSL, Hormone-sensitive lipase; H&E, Hematoxylin and eosin; IL-6/*IL-6*, Interleukin-6; IHC, Immunohistochemical; IPGTT, Intraperitoneal glucose tolerance test; KEGG, Kyoto Encyclopedia of Genes and Genomes; LC-MS/MS, Liquid chromatography–tandem mass spectrometry; LDL-C, Low-density lipoprotein Cholesterol; LIPEA, Lipid pathway enrichment analysis; *Lipe*, Lipase E, hormone sensitive type; *Pnpla2*, Patatin-like phospholipase domain containing 2; *Ppargc1α*, Proliferator-activated receptor gamma coactivator 1-alpha; *Prdm16*, PR domain containing 16; *Lpcat1*, Lysophosphatidylcholine acyltransferase 1; *Lpcat3*, Lysophosphatidylcholine acyltransferase 3; NASH, Non-alcoholic steatohepatitis; PKC, Protein kinase C; PCA, Principal component analysis; *Pemt*, Phosphatidylethanolamine N-methyltransferase; RT-qPCR, Reverse transcription-quantitative PCR; SAT, Subcutaneous adipose tissue; STZ, Streptozotocin; TC, Total cholesterol; TNF-α/*TNF-α*, Tumor necrosis factor alpha; *Ucp1*, uncoupling protein 1; VAT, Visceral adipose tissue; WAT, White adipose tissue; WAT index, WAT-to-body weight ratio.

Availability of Data and Materials

The data presented in this study are available on request from the corresponding author.

Author Contributions

XC and YY designed the research study. XC, BT performed the research. XC, ZL, PG, YX, YY analyzed the data. XC wrote the first draft of manuscript. All authors contributed to editorial changes in the manuscript. All authors read and approved the final manuscript. All authors have participated sufficiently in the work and agreed to be accountable for all aspects of the work.

Ethics Approval and Consent to Participate

The study, conducted in accordance with the ARRIVE guidelines (https://arriveguidelines.org) and the Guidelines for Ethical Review of Laboratory Animal Welfare (GB/T 35892-2018), was approved by the Medical Ethics Committee of the Second Affiliated Hospital of Harbin Medical University (Registration Number YJSDW2024-026).

Acknowledgment

The authors gratefully acknowledge the research support provided by the Scientific Research Center of the Second Affiliated Hospital of Harbin Medical University, the Key Laboratory of Myocardial Ischemia (Harbin Medical University), and the State Key Laboratory of Liver Research (The University of Hong Kong). We thank them for providing the experimental facilities and technical support essential for this work.

Funding

This work was supported by the National Natural Science Foundation of China (Grant No. 82300921).

Conflicts of Interest

The authors declare no conflicts of interest.

References

[1] World Obesity Federation. World Obesity Atlas 2025. 2025. Available at: https://data.worldobesity.org/publications/?cat=23 (Accessed: 13 November 2025).

[2] Jayedi A, Soltani S, Motlagh SZT, Emadi A, Shahinfar H, Moosavi H, et al. Anthropometric and adiposity indicators and risk of type 2 diabetes: systematic review and dose-response meta-analysis of cohort studies. BMJ (Clinical Research Ed.). 2022; 376: e067516. https://doi.org/10.1136/bmj-2021-067516

[3] Chait A, den Hartigh LJ. Adipose Tissue Distribution, Inflammation and Its Metabolic Consequences, Including Diabetes and Cardiovascular Disease. Frontiers in Cardiovascular Medicine. 2020; 7: 22. https://doi.org/10.3389/fcvm.2020.00022

[4] Lyu K, Zhang D, Song J, Li X, Perry RJ, Samuel VT, et al. Short-term overnutrition induces white adipose tissue insulin resistance through sn-1,2-diacylglycerol/PKCε/insulin receptor Thr1160 phosphorylation. JCI Insight. 2021; 6: e139946. https://doi.org/10.1172/jci.insight.139946

[5] Tuncman G, Hirosumi J, Solinas G, Chang L, Karin M, Hotamisligil GS. Functional in vivo interactions between JNK1 and JNK2 isoforms in obesity and insulin resistance. Proceedings of the National Academy of Sciences of the United States of America. 2006; 103: 10741–10746. https://doi.org/10.1073/pnas.0603509103

[6] American Diabetes Association Professional Practice Committee for Diabetes. 9. Pharmacologic Approaches to Glycemic Treatment: Standards of Care in Diabetes-2026. Diabetes Care. 2026; 49: S183–S215. https://doi.org/10.2337/dc26-S009.

[7] Bertoccini L, Baroni MG. GLP-1 Receptor Agonists and SGLT2 Inhibitors for the Treatment of Type 2 Diabetes: New Insights and Opportunities for Cardiovascular Protection. Advances in Experimental Medicine and Biology. 2021; 1307: 193–212. https://doi.org/10.1007/5584_2020_494

[8] Joseph J. The Impact of Semaglutide on Metabolic Syndrome: A Case Report. Cureus. 2025; 17: e87223. https://doi.org/10.7759/cureus.87223

[9] Gao X, Sun H, Wei Y, Niu J, Hao S, Sun H, et al. Protective effect of melatonin against metabolic disorders and neuropsychiatric injuries in type 2 diabetes mellitus mice. Phytomedicine : International Journal of Phytotherapy and Phytopharmacology. 2024; 131: 155805. https://doi.org/10.1016/j.phymed.2024.155805.

[10] Zhang K, Pan H, Wang L, Yang H, Zhu H, Gong F. Adipose Tissue Insulin Resistance is Closely Associated with Metabolic Syndrome in Northern Chinese Populations. Diabetes, Metabolic Syndrome and Obesity : Targets and Therapy. 2021; 14: 1117–1128. https://doi.org/10.2147/DMSO.S291350

[11] Semnani-Azad Z, Connelly PW, Bazinet RP, Retnakaran R, Jenkins DJA, Harris SB, et al. Adipose Tissue Insulin Resistance Is Longitudinally Associated With Adipose Tissue Dysfunction, Circulating Lipids, and Dysglycemia: The PROMISE Cohort. Diabetes Care. 2021; 44: 1682–1691. https://doi.org/10.2337/dc20-1918

[12] Jiang S, Li H, Zhang L, Mu W, Zhang Y, Chen T, et al. Generic Diagramming Platform (GDP): a comprehensive database of high-quality biomedical graphics. Nucleic Acids Research. 2025; 53: D1670–D1676. https://doi.org/10.1093/nar/gkae973

[13] Ahmad E, Lim S, Lamptey R, Webb DR, Davies MJ. Type 2 diabetes. Lancet (London, England). 2022; 400: 1803–1820. https://doi.org/10.1016/S0140-6736(22)01655-5

[14] Młynarska E, Czarnik W, Dzieża N, Jędraszak W, Majchrowicz G, Prusinowski F, et al. Type 2 Diabetes Mellitus: New Pathogenetic Mechanisms, Treatment and the Most Important Complications. International Journal of Molecular Sciences. 2025; 26: 1094. https://doi.org/10.3390/ijms26031094

[15] Xie C, Yuan Y, Wang Y, Qi C, Wang W, An C, et al. Beyond Discrete Diagnoses: Conceptualizing Obesity-associated Metabolic Disorders as a Unified, Dynamic Continuum. Current Obesity Reports. 2025; 14: 81. https://doi.org/10.1007/s13679-025-00673-5

[16] Rodbard HW, Lingvay I, Reed J, de la Rosa R, Rose L, Sugimoto D, et al. Semaglutide Added to Basal Insulin in Type 2 Diabetes (SUSTAIN 5): A Randomized, Controlled Trial. The Journal of Clinical Endocrinology and Metabolism. 2018; 103: 2291–2301. https://doi.org/10.1210/jc.2018-00070

[17] Cantini G, Mannucci E, Luconi M. Perspectives in GLP-1 Research: New Targets, New Receptors. Trends in Endocrinology and Metabolism: TEM. 2016; 27: 427–438. https://doi.org/10.1016/j.tem.2016.03.017

[18] Rodríguez Jiménez B, Rodríguez de Vera Gómez P, Belmonte Lomas S, Mesa Díaz ÁM, Caballero Mateos I, Galán I, et al. Transforming body composition with semaglutide in adults with obesity and type 2 diabetes mellitus. Frontiers in Endocrinology. 2024; 15: 1386542. https://doi.org/10.3389/fendo.2024.1386542

[19] Li J, Hou H, Zhang Y, Li J. Multimorbidity patterns and their associated factors among patients with type 2 diabetes in China: A hospital-based observational study. Heliyon. 2025; 11: e42905. https://doi.org/10.1016/j.heliyon.2025.e42905

[20] Tiwaskar M, Hwu CM, Lim M, Bhandary A, Chang I. Treatment Preferences for Novel Type 2 Diabetes Oral Medications: Insights from the Asian Diabetes Patient Preference Study. Diabetes Therapy: Research, Treatment and Education of Diabetes and Related Disorders. 2025; 16: 1841–1859. https://doi.org/10.1007/s13300-025-01770-3.

[21] Wong ND, Sattar N. Cardiovascular risk in diabetes mellitus: epidemiology, assessment and prevention. Nature Reviews. Cardiology. 2023; 20: 685–695. https://doi.org/10.1038/s41569-023-00877-z

[22] Di Folco U, Vallecorsa N, Nardone MR, Pantano AL, Tubili C. Effects of semaglutide on cardiovascular risk factors and eating behaviors in type 2 diabetes. Acta Diabetologica. 2022; 59: 1287–1294. https://doi.org/10.1007/s00592-022-01936-6

[23] Gabery S, Salinas CG, Paulsen SJ, Ahnfelt-Rønne J, Alanentalo T, Baquero AF, et al. Semaglutide lowers body weight in rodents via distributed neural pathways. JCI Insight. 2020; 5: e133429. https://doi.org/10.1172/jci.insight.133429

[24] Wong ND, Karthikeyan H, Fan W. US Population Eligibility and Estimated Impact of Semaglutide Treatment on Obesity Prevalence and Cardiovascular Disease Events. Cardiovascular Drugs and Therapy. 2025; 39: 75–84. https://doi.org/10.1007/s10557-023-07488-3

[25] Bays H, Mandarino L, DeFronzo RA. Role of the adipocyte, free fatty acids, and ectopic fat in pathogenesis of type 2 diabetes mellitus: peroxisomal proliferator-activated receptor agonists provide a rational therapeutic approach. The Journal of Clinical Endocrinology and Metabolism. 2004; 89: 463–478. https://doi.org/10.1210/jc.2003-030723

[26] Diraison F, Beylot M. Role of human liver lipogenesis and reesterification in triglycerides secretion and in FFA reesterification. The American Journal of Physiology. 1998; 274: E321–7. https://doi.org/10.1152/ajpendo.1998.274.2.E321

[27] McLaughlin T, Lamendola C, Liu A, Abbasi F. Preferential fat deposition in subcutaneous versus visceral depots is associated with insulin sensitivity. The Journal of Clinical Endocrinology and Metabolism. 2011; 96: E1756–60. https://doi.org/10.1210/jc.2011-0615

[28] Lomonaco R, Ortiz-Lopez C, Orsak B, Webb A, Hardies J, Darland C, et al. Effect of adipose tissue insulin resistance on metabolic parameters and liver histology in obese patients with nonalcoholic fatty liver disease. Hepatology (Baltimore, Md.). 2012; 55: 1389–1397. https://doi.org/10.1002/hep.25539

[29] Teixidor-Deulofeu J, Blid Sköldheden S, Font-Gironès F, Feješ

A, Ruud J, Engström Ruud L. Semaglutide effects on energy balance are mediated by Adcyap1+ neurons in the dorsal vagal complex. Cell Metabolism. 2025; 37: 1530–1546.e6. https://doi.org/10.1016/j.cmet.2025.04.018

[30] Byun S, Sotzen MR, Knappenberger MA, Bento MT, Asker M, Olekanma DI, et al. Advantage of Semaglutide: Comprehensive Analysis of Metabolic Impact of Semaglutide-Treated and Pair-Fed Rats. Comprehensive Physiology. 2025; 15: e70083. https://doi.org/10.1002/cph4.70083

[31] Yang J, Ren J, Song J, Liu F, Wu C, Wang X, et al. Glucagon-like peptide 1 regulates adipogenesis in 3T3-L1 preadipocytes. International Journal of Molecular Medicine. 2013; 31: 1429–1435. https://doi.org/10.3892/ijmm.2013.1350

[32] Yan K. Recent advances in the effect of adipose tissue inflammation on insulin resistance. Cellular Signalling. 2024; 120: 111229. https://doi.org/10.1016/j.cellsig.2024.111229

[33] Jiang YN, Gao Y, Zhang YS, Min CY, Shen LT, Yan WF, et al. Aggravating effect of abnormal low-density protein cholesterol level on coronary atherosclerotic plaque in type 2 diabetes mellitus patients assessed by coronary computed tomography angiography. Cardiovascular Diabetology. 2024; 23: 234. https://doi.org/10.1186/s12933-024-02304-0

[34] O'Rourke RW, White AE, Metcalf MD, Olivas AS, Mitra P, Larison WG, et al. Hypoxia-induced inflammatory cytokine secretion in human adipose tissue stromovascular cells. Diabetologia. 2011; 54: 1480–1490. https://doi.org/10.1007/s00125-011-2103-y

[35] Todosenko N, Yurova K, Khaziakhmatova O, Vulf M, Malashchenko V, Komar A, et al. The Role of (Nuclear) Lipid Droplets in the Pathogenesis of Metabolic Syndrome. Frontiers in Bioscience (Landmark Edition). 2025; 30: 26742. https://doi.org/10.31083/FBL26742

[36] Bendotti G, Montefusco L, Lunati ME, Usuelli V, Pastore I, Lazzaroni E, et al. The anti-inflammatory and immunological properties of GLP-1 Receptor Agonists. Pharmacological Research. 2022; 182: 106320. https://doi.org/10.1016/j.phrs.2022.106320

[37] Miranda AMA, McAllan L, Mazzei G, Andrew I, Davies I, Ertugrul M, et al. Selective remodelling of the adipose niche in obesity and weight loss. Nature. 2025; 644: 769–779. https://doi.org/10.1038/s41586-025-09233-2

[38] Drucker DJ. Mechanisms of Action and Therapeutic Application of Glucagon-like Peptide-1. Cell Metabolism. 2018; 27: 740–756. https://doi.org/10.1016/j.cmet.2018.03.001

[39] Barbarroja N, Lopez-Pedrera C, Garrido-Sanchez L, Mayas MD, Oliva-Olivera W, Bernal-Lopez MR, et al. Progression from high insulin resistance to type 2 diabetes does not entail additional visceral adipose tissue inflammation. PloS One. 2012; 7: e48155. https://doi.org/10.1371/journal.pone.0048155

[40] Lee YS, Park MS, Choung JS, Kim SS, Oh HH, Choi CS, et al. Glucagon-like peptide-1 inhibits adipose tissue macrophage infiltration and inflammation in an obese mouse model of diabetes. Diabetologia. 2012; 55: 2456–2468. https://doi.org/10.1007/s00125-012-2592-3

[41] Guo C, Huang T, Chen A, Chen X, Wang L, Shen F, et al. Glucagon-like peptide 1 improves insulin resistance in vitro through anti-inflammation of macrophages. Brazilian Journal of Medical and Biological Research = Revista Brasileira De Pesquisas Medicas E Biologicas. 2016; 49: e5826. https://doi.org/10.1590/1414-431X20165826

[42] Montserrat-de la Paz S, Pérez-Pérez A, Vilariño-García T, Jiménez-Cortegana C, Muriana FJG, Millán-Linares MC, et al. Nutritional modulation of leptin expression and leptin action in obesity and obesity-associated complications. The Journal of Nutritional Biochemistry. 2021; 89: 108561. https://doi.org/10.1016/j.jnutbio.2020.108561

[43] Tilg H, Ianiro G, Gasbarrini A, Adolph TE. Adipokines: masterminds of metabolic inflammation. Nature Reviews. Immunology. 2025; 25: 250–265. https://doi.org/10.1038/s41577-024-01103-8

[44] Huang CX, Siwan E, Baker CJ, Wei Z, Shinko D, McGuire HM, et al. Uncovering Sex-Related Differences in Skin Macrophage Polarization During Wound Healing in Diabetic Mice. Frontiers in Bioscience (Landmark Edition). 2025; 30: 27113. https://doi.org/10.31083/FBL27113

[45] Gemmink A, Daemen S, Brouwers B, Hoeks J, Schaart G, Knoops K, et al. Decoration of myocellular lipid droplets with perilipins as a marker for in vivo lipid droplet dynamics: A super-resolution microscopy study in trained athletes and insulin resistant individuals. Biochimica et Biophysica Acta. Molecular and Cell Biology of Lipids. 2021; 1866: 158852. https://doi.org/10.1016/j.bbalip.2020.158852

[46] Long C, Li Z, Jiang L, Yang X, Deng S, Jiang Y, et al. Lipid droplet dynamics in type 2 diabetes and its complications: pathophysiological insights and therapeutic options. Lipids in Health and Disease. 2025; 24: 284. https://doi.org/10.1186/s12944-025-02747-8

[47] Herrera-Marcos LV, Martínez-Beamonte R, Arnal C, Barranquero C, Puente-Lanzarote JJ, Herrero-Continente T, et al. Dietary squalene supplementation decreases triglyceride species and modifies phospholipid lipidomic profile in the liver of a porcine model of non-alcoholic steatohepatitis. The Journal of Nutritional Biochemistry. 2023; 112: 109207. https://doi.org/10.1016/j.jnutbio.2022.109207

[48] Zhou M, Liu X, Wu Y, Xiang Q, Yu R. Liver Lipidomics Analysis Revealed the Protective mechanism of Zuogui Jiangtang Qinggan Formula in type 2 diabetes mellitus with non-alcoholic fatty liver disease. Journal of Ethnopharmacology. 2024; 329: 118160. https://doi.org/10.1016/j.jep.2024.118160

[49] Pei Y, Song Y, Wang B, Lin C, Yang Y, Li H, et al. Integrated lipidomics and RNA sequencing analysis reveal novel changes during 3T3-L1 cell adipogenesis. PeerJ. 2022; 10: e13417. https://doi.org/10.7717/peerj.13417

[50] Sim JA, Kim J, Yang D. Beyond Lipid Signaling: Pleiotropic Effects of Diacylglycerol Kinases in Cellular Signaling. International Journal of Molecular Sciences. 2020; 21: 6861. https://doi.org/10.3390/ijms21186861

[51] Masenga SK, Kabwe LS, Chakulya M, Kirabo A. Mechanisms of Oxidative Stress in Metabolic Syndrome. International Journal of Molecular Sciences. 2023; 24: 7898. https://doi.org/10.3390/ijms24097898

[52] Szendroedi J, Yoshimura T, Phielix E, Koliaki C, Marcucci M, Zhang D, et al. Role of diacylglycerol activation of PKCθ in lipid-induced muscle insulin resistance in humans. Proceedings of the National Academy of Sciences of the United States of America. 2014; 111: 9597–9602. https://doi.org/10.1073/pnas.1409229111

[53] van der Veen JN, Lingrell S, McCloskey N, LeBlond ND, Galleguillos D, Zhao YY, et al. A role for phosphatidylcholine and phosphatidylethanolamine in hepatic insulin signaling. FASEB Journal : Official Publication of the Federation of American Societies for Experimental Biology. 2019; 33: 5045–5057. https://doi.org/10.1096/fj.201802117R

[54] Tian Y, Mehta K, Jellinek MJ, Sun H, Lu W, Shi R, et al. Hepatic Phospholipid Remodeling Modulates Insulin Sensitivity and Systemic Metabolism. Advanced Science (Weinheim, Baden-Wurttemberg, Germany). 2023; 10: e2300416. https://doi.org/10.1002/advs.202300416

[55] Guo C, Han X, Zhang T, Zhang H, Li X, Zhou X, et al. Lipidomic analyses reveal potential biomarkers for predicting death and heart failure after acute myocardial infarction. Clinica Chimica Acta; International Journal of Clinical Chemistry. 2024; 562: 119892. https://doi.org/10.1016/j.cca.2024.119892

[56] Kayser BD, Lhomme M, Prifti E, Da Cunha C, Marquet F, Chain F, et al. Phosphatidylglycerols are induced by gut dysbiosis and inflammation, and favorably modulate adipose tissue remodeling in obesity. FASEB Journal : Official Publication of the Federation of American Societies for Experimental Biology. 2019; 33: 4741–4754. https://doi.org/10.1096/fj.201801897R

[57] Patel V, Joharapurkar A, Kshirsagar S, Sutariya B, Patel M, Patel H, et al. Central administration of coagonist of GLP-1 and glucagon receptors improves dyslipidemia. Biomedicine & Pharmacotherapy = Biomedecine & Pharmacotherapie. 2018; 98: 364–371. https://doi.org/10.1016/j.biopha.2017.12.068

[58] Butovich IA. Cholesteryl esters as a depot for very long chain fatty acids in human meibum. Journal of Lipid Research. 2009; 50: 501–513. https://doi.org/10.1194/jlr.M800426-JLR200

[59] Kawaguchi T, Itou M, Taniguchi E, Sata M. Exendin-4, a glucagon-like peptide-1 receptor agonist, modulates hepatic fatty acid composition and Δ-5-desaturase index in a murine model of non-alcoholic steatohepatitis. International Journal of Molecular Medicine. 2014; 34: 782–787. https://doi.org/10.3892/ijmm.2014.1826

[60] Yan W, Cui X, Guo T, Liu N, Wang Z, Sun Y, et al. ALOX15 Aggravates Metabolic Dysfunction-Associated Steatotic Liver Disease in Mice with Type 2 Diabetes via Activating the PPARγ/CD36 Axis. Antioxidants & Redox Signaling. 2025; 43: 37–55. https://doi.org/10.1089/ars.2024.0670

[61] Xu F, Lin B, Zheng X, Chen Z, Cao H, Xu H, et al. GLP-1 receptor agonist promotes brown remodelling in mouse white adipose tissue through SIRT1. Diabetologia. 2016; 59: 1059–1069. https://doi.org/10.1007/s00125-016-3896-5

[62] Zhou J, Poudel A, Chandramani-Shivalingappa P, Xu B, Welchko R, Li L. Liraglutide induces beige fat development and promotes mitochondrial function in diet induced obesity mice partially through AMPK-SIRT-1-PGC1-α cell signaling pathway. Endocrine. 2019; 64: 271–283. https://doi.org/10.1007/s12020-018-1826-7

[63] Zhao L, Zhu C, Lu M, Chen C, Nie X, Abudukerimu B, et al. The key role of a glucagon-like peptide-1 receptor agonist in body fat redistribution. The Journal of Endocrinology. 2019; 240: 271–286. https://doi.org/10.1530/JOE-18-0374

[64] Sun L, Shang B, Lv S, Liu G, Wu Q, Geng Y. Effects of semaglutide on metabolism and gut microbiota in high-fat diet-induced obese mice. Frontiers in Pharmacology. 2025; 16: 1562896. https://doi.org/10.3389/fphar.2025.1562896